

Joussame

CNRS - Université Pierre et Marie Curie - Université Versailles-Saint-Quentin
CEA - ORSTOM - Ecole Normale Supérieure - Ecole Polytechnique

Institut Pierre Simon Laplace

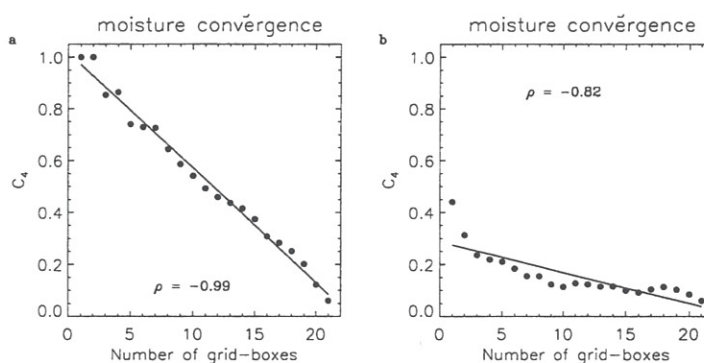
des sciences de l'Environnement Global

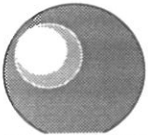
Notes du Pôle de Modélisation

Sensitivity of the hydrological cycle to the parameterization of soil hydrology in a GCM

Agnès Ducharne, Katia Laval and Jan Polcher

Laboratoire de Météorologie Dynamique du CNRS, Paris,
France



 I P S L	CNRS - Université Pierre et Marie Curie - Université Versailles-Saint-Quentin CEA - CNES - ORSTOM - Ecole Normale Supérieure - Ecole Polytechnique
	Institut Pierre Simon Laplace des Sciences de l'Environnement Global
	CETP - CFR - LMCE - LMD - LODYC - LPCM - SA
Université Pierre-et-Marie-Curie B 102 - T15-E5 - 4, Place Jussieu 75252 Paris Cedex 05 (France) Tél : (33) 01 44 27 39 83 Fax : (33) 01 44 27 37 76	Université Versailles-Saint-Quentin Collège Vauban, 47 Boulevard Vauban 78047 Guyancourt Cedex (France) Tél : (33) 01 39 25 58 17 Fax : (33) 01 39 25 58 22

Paris, le 25 Février 1998

Cher(e) collègue,

Le Pôle Modélisation de l'ISPL a mis en place une note interne à large diffusion auprès de la communauté nationale et internationale. Cette note a pour finalité de mieux faire connaître à l'intérieur et à l'extérieur de l'Institut les travaux scientifiques dont la problématique recouvre les actions du Pôle Modélisation de l'ISPL. Ces actions s'articulent autour de l'étude du climat global, avec une attention plus particulière sur les processus de couplage, à savoir dans un premier temps ceux intervenant dans les interactions océan/atmosphère/glace, chimie/atmosphère, biogéochimie/océan, et hydrologie/végétation/atmosphère.

Ces notes sont du niveau de papiers soumis dans des revues de rang A. Elles sont soumises à un dépôt légal, avec numéro ISSN. Cette démarche apporte une certaine rapidité dans la diffusion des résultats de nos recherches (un gain de l'ordre de un à deux ans) et permet de pouvoir référencer ces résultats avant qu'ils ne soient effectivement publiés dans la presse internationale.

Une expertise rapide, qui ne peut se substituer à celle effectuée par les journaux, est organisée en interne. Une fois cette étape franchie, les notes seront éditées par l'IPSL et envoyées à un nombre assez important de collègues français et étrangers (liste de l'ordre de 150 personnes dans un premier temps). Un certain nombre d'exemplaires sera mis à disposition des auteurs.

Si vous souhaitez soumettre un papier aux notes Pôle Modélisation IPSL, il vous suffit d'envoyer le document aux éditeurs (pour l'instant Laurent Mémery, LODYC et Jan Polcher, LMD). Etant donné que la liste de ces notes va continuellement être mise à jour sur le serveur WWW du pôle, il nous faudrait en outre un certain nombre d'informations par e-mail, à savoir :

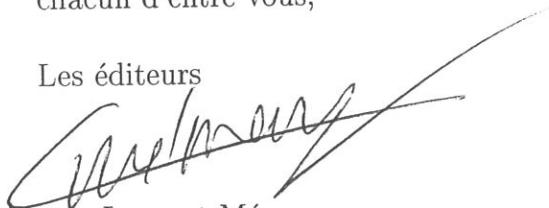
- Titre
- Auteurs
- Laboratoires
- Figure de la couverture de la note (PostScript, JPEG, TIFF)

- Abstract en anglais
- Résumé en français

Pour ce qui concerne l'article lui même, le plus simple est de tout envoyer électroniquement sous PostScript. A noter que les figures seront éditées exclusivement en noir et blanc, et qu'elles doivent impérativement être numérotées.

En espérant que cette démarche recueille l'assentiment et la participation de chacun d'entre vous,

Les éditeurs

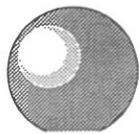


Laurent Mémery
LODYC
lm@lodyc.jussieu.fr
lmlod@ipsl.jussieu.fr
Tel: 01 44 27 49 66
Fax: 01 44 27 71 59
LODYC/IPSL
Univ. Pierre et Marie Curie
Case 100
4 Place Jussieu
75252 Paris Cedex 5



Jan Polcher
LMD
polcher@lmd.jussieu.fr

Tel: 01 44 27 47 63
Fax: 01 44 27 62 72
LMD/IPSL
Univ. Pierre et Marie Curie
Case 99
4 Place Jussieu
75252 Paris Cedex 5

 I P S L	<p align="center"> CNRS - Université Pierre et Marie Curie - Université Versailles-Saint-Quentin CEA - CNES - ORSTOM - Ecole Normale Supérieure - Ecole Polytechnique Institut Pierre Simon Laplace des Sciences de l'Environnement Global CETP - CFR - LMCE - LMD - LODYC - LPCM - SA </p>
Université Pierre-et-Marie-Curie B 102 - T15-E5 - 4, Place Jussieu 75252 Paris Cedex 05 (France) Tél : (33) 01 44 27 39 83 Fax : (33) 01 44 27 37 76	<p align="right"> Université Versailles-Saint-Quentin College Vauban, 47 Boulevard Vauban 78047 Guyancourt Cedex (France) Tél : (33) 01 39 25 58 17 Fax : (33) 01 39 25 58 22 </p>

Sensitivity of the hydrological cycle to the parameterization of soil hydrology in a GCM

Agnès Ducharne, Katia Laval and Jan Polcher

Laboratoire de Météorologie Dynamique du CNRS, Paris,
France

<p align="center"> Janvier 1998 Note n° 1 </p>

Sensitivity of the hydrological cycle to the parameterization of soil hydrology in a GCM

Agnès Ducharne, Katia Laval and Jan Polcher

Laboratoire de Météorologie Dynamique du CNRS, Paris, France

Address of Correspondence

Katia Laval

Laboratoire de Météorologie Dynamique du CNRS

Université Pierre et Marie Curie - BP 99

4, place Jussieu

75252 PARIS cedex 05

FRANCE

TEL: (33) 01.44.32.22.44

FAX: (33) 01.43.27.62.72

e-mail: laval@lmd.jussieu.fr

Abstract

The sensitivity of the hydrological cycle to soil hydrology is investigated with the LMD GCM. The reference simulation includes the land-surface scheme SECHIBA, with a two-reservoir scheme for soil water storage and runoff at saturation. Are studied a non-linear drainage parameterization, and a distributed surface runoff parameterization, accounting for the subgrid scale variability (SSV) of soil moisture capacity, through a distribution with a shape parameter b .

GCM results show that the drainage parameterization induces significant reductions in soil moisture and evaporation rate compared to the reference simulation. They are related to changes in moisture convergence in the tropics, and to a precipitation decrease in the extratropics. When drainage is implemented, the effect of the SSV parameterization ($b=0.2$) is also to reduce soil moisture and evaporation rate compared to the simulation with drainage only. These changes are much smaller than the former, but the sensitivity of the hydrological cycle to the SSV parameterization is shown to be larger in dry periods, and to be enhanced by an increase of the shape parameter b . The comparison of simulated total runoffs with observed data shows that the soil hydrological parameterizations does not reduce the GCM systematic errors in the annual water balance, but that they can improve the representation of the total runoff annual cycle.

1 Introduction

General Circulation Models (GCMs), which are designed to understand climate variations, must simulate rather realistically the hydrological budget of the atmosphere. It implies that, in each grid-box of the model, precipitation and evaporation rates are computed accurately. The question addressed here is the evolution of the precipitated water when it reaches land surface. How much is evaporated ? What part is infiltrated and what part does run off ? The first scheme that took hydrological processes into account in GCMs was the bucket model (Manabe 1969). It has two simple assumptions. One is to compute the evaporation rate by multiplying the potential rate by an aridity coefficient, which is a simple function of total soil moisture content. The second one is to infiltrate all the water reaching the soil until saturation ; afterwards, runoff takes place to remove the excess water at the surface.

It has been shown that this scheme induced too much dryness during summer, and some attempts were carried out to compute differently the potential evaporation rate (Milly 1992; Laval et al. 1984), retaining a single reservoir to define soil moisture content as in the bucket model. Attempts were also made in GCMs to represent the characteristics of vegetation to compute evapotranspiration, which is the sum of transpiration by vegetation, interception loss from wet foliage, and soil evaporation. The vegetation is not uniform over a grid-box, and there were two ways of introducing this heterogeneity : one was to define a mean value of the parameters of the vegetative cover, as in SiB (Sellers et al. 1986) and BATS (Dickinson 1984). Another way was to define a mosaic of vegetation types inside the grid-box, to compute for each of them the water exchanges of land surface with the atmosphere, and to average the fluxes (Ducoudré et al. 1993; Koster and Suarez 1992).

Attempts were also made to define infiltration and runoff in a more realistic way than in the bucket model. Those processes are variable over a spatial scale much smaller than the GCM grid scale, because of the high spatial variability of rainfall and clouds, soil properties and topography. Since it is not possible yet to increase the model grid scale by the required orders of magnitude, it is important to find methods to account for the processes occurring at the subgrid scales in the models. One method is based on statistical distribution functions. For instance, Warrilow et al. (1986) used an exponential distribution to define the effect of rainfall heterogeneity on runoff in the UKMO GCM. Entekhabi and Eagleson (1989) published a land surface hydrology parameterization in which both precipitation and soil moisture were statistically distributed over

the grid mesh. This parameterization was tested in the GISS-II GCM (Johnson et al. 1993). With a much simpler model than the one defined by Entekhabi and Eagleson (1989), Dümenil and Todini (1992) and Wood et al. (1992) distributed soil moisture capacity inside a model grid-box (Arno and VIC models) to define the subgrid scale variability (SSV) of surface runoff. The accounting for soil moisture heterogeneity was originally developed in catchment rainfall-runoff models (Bergström and Forsman 1973; Zhao 1977; Todini 1988). Both the VIC and Arno models include a drainage term together with the subgrid scale variability of surface runoff, and they were implemented in GCMs. In particular, the VIC model was introduced in the GFDL GCM, and compared to the bucket model (Stamm et al. 1994). The VIC model was shown to induce significant changes in the simulated hydrological budget, but it is difficult to distinguish between the effects of the drainage and the subgrid scale variability of surface runoff.

In the present study, we introduce separately the subgrid scale variability of surface runoff and a drainage term in the LMD¹ GCM, in order to quantify the sensitivity of climate to each of these processes. Section 2 presents the hydrological parameterizations, and shows the importance of the distribution shape parameter for the response to the SSV parameterization. Section 3 presents the numerical experiments. Section 4 gives a detailed study of the sensitivity of the GCM, and especially of surface runoff, to the subgrid scale variability of soil moisture capacity, with a selected value of the shape parameter, and with drainage implemented. It is compared to the sensitivity to drainage alone in section 5. Section 6 assesses the influence of the shape parameter for the sensitivity of the GCM to the SSV parameterization, in comparison with the sensitivity to drainage. It also includes a comparison of the GCM results with observed data. The conclusions of the work are given in section 7.

2 Description of land-surface hydrology

2.1 The land-surface scheme SECHIBA

Land surface hydrology is described in the LMD GCM by the land-surface scheme SECHIBA (Ducoudré et al. 1993), which defines a mosaic of bare soil and up to seven vegetation types in a grid-box. The total evaporation is computed as the weighted average of snow sublimation, bare soil evaporation, transpiration and interception loss from each of the tiles in a grid-box. Evapotran-

¹Laboratoire de Météorologie Dynamique

spiration is controlled by a set of resistances, defined as in Polcher and Laval (1994), and by an aridity coefficient that accounts for the influence of soil moisture. The same aridity coefficient is used for each of the tiles in a grid-box as they share the same soil moisture.

The evolution of soil moisture is computed with an original two-reservoir soil model, based on Choissnel's ideas (Choissnel et al. 1995). The depth of active soil is one meter. The storage capacity, \bar{c} , is globally equal to 150 kg.m^{-2} . An exception exists over deserts, where it is 30 kg.m^{-2} . The upper reservoir has a variable depth, ranging from 0 to 10 cm. Rainfall can either create the upper reservoir, in which case it is saturated, or fill it. This reservoir can deepen when it is saturated, until it reaches its maximum depth. Any water input beyond this point goes to the lower reservoir. Evapotranspiration is extracted from the upper reservoir when it exists, and otherwise from the lower one. In all cases, the aridity coefficient is taken as the minimum of the values computed with the moistures of the upper and lower reservoirs. Evapotranspiration occurs therefore at the potential rate when the upper reservoir has just been created.

The excess water when the whole soil column is saturated defines the runoff, like in the bucket scheme (Manabe 1969). This basic form of runoff is uniformly distributed over a grid-box, and flows over the soil surface. It will therefore be referred to as the uniform surface runoff.

2.2 Drainage parameterization

Drainage between the two soil reservoirs and at the bottom of the soil is modified from the one defined by Dümenil and Todini (1992) for their one-reservoir soil model. Drainage from a reservoir depends on its water content in a non-linear form : drainage D_i from i -th reservoir is governed by the following set of equations

$$D_i = D_i^{\min} \frac{W_i}{W_i^{\max}} \quad \text{if } W_i < W_i^{\lim} \quad (1)$$

$$D_i = D_i^{\min} \frac{W_i}{W_i^{\max}} + (D_i^{\max} - D_i^{\min}) \left(\frac{W_i - W_i^{\lim}}{W_i^{\max} - W_i^{\lim}} \right)^{d_i} \quad \text{if } W_i \geq W_i^{\lim} \quad (2)$$

where i indexes the reservoir. W_i is the water content of the i -th reservoir and W_i^{\max} is its maximum water content. It is computed as $W_i^{\max} = h_i \bar{c}$, where h_i is the depth of the reservoir (m) and \bar{c} is the maximum water content of the whole soil column (kg.m^{-3}). Note that the water drained from the upper reservoir goes to the lower reservoir, and increases the water content of the latter.

In both reservoirs, D_i^{max} is 100 times higher than D_i^{min} , implying a strong increase of drainage when the water content of the reservoir goes above the threshold W_i^{lim} . In the lower reservoir, $D_i^{min}=0.0005 \text{ mm.h}^{-1}$ and $D_i^{max}=0.05 \text{ mm.h}^{-1}$. The values of D_i^{min} and D_i^{max} are greater for the upper reservoir ($D_i^{min}=0.002 \text{ mm.h}^{-1}$ and $D_i^{max}=0.2 \text{ mm.h}^{-1}$). This is designed to accelerate the vanishing of the upper layer, and facilitate potential rate evapotranspiration after a shower (section 2.1). The threshold soil moisture W_i^{lim} and d_i are identical in the two reservoirs : $W_i^{lim} = 0.75W_i^{max}$, and $d_i=1.5$. The above parameters lie in the range of the values cited in previous studies using this “two-speed” drainage parameterization (Dümenil and Todini 1992; Rowntree and Lean 1994).

The drainage from the upper reservoir can be seen as a diffusion between the two reservoirs. In the remainder of this paper, when not specified, drainage will then denote the drainage at the bottom of the soil column.

2.3 Surface runoff parameterization

Because of the subgrid scale variability of storage capacity, one can divide every continental grid-box into local storage elements, characterized by their local storage capacity c (ranging from 0 to a maximum value c_{max}). The storage capacity of the whole grid-box \bar{c} is the average of all the local storage capacities. F is the distribution function of c for a grid-box, and $F(c^*)$ gives the fraction of the grid-box in which storage capacity is less than or equal to c^* :

$$F(c^*) = 1 - \left(1 - \frac{c^*}{c_{max}}\right)^b \quad (3)$$

where b is a shape parameter. With this distribution, the maximum local storage capacity c_{max} is related to the mean storage capacity in the grid-box \bar{c} :

$$c_{max} = (b + 1) \bar{c} \quad (4)$$

The evolution of W , the total water content in the grid-box, is given by :

$$\frac{\partial W}{\partial t} = P_{soil} + M - E - R - D \quad (5)$$

where t is time, P_{soil} is the rainfall reaching the soil, M is snowmelt, E evapotranspiration, R surface runoff and D drainage. The computation sequence in SECHIBA is such that drainage is computed after surface runoff. In a timestep, the surface runoff rate is then independent of

the drainage rate. The evaporation rate is on the opposite computed before the surface runoff rate, and the water input at the surface for soil hydrology is the net precipitation P_n :

$$P_n = P_{soil} + M - E \quad (6)$$

P_n is homogeneous through the grid-box, because evaporation is computed under the assumption of homogeneous soil moisture and aridity coefficient. We define \mathcal{R} and \mathcal{P}_n as the amounts during a timestep Δt corresponding to the rates R and P_n respectively ; W_t and $W_{t+\Delta t}$ give the total water content in the grid-box, at the beginning and the end of the timestep respectively. Then :

$$\mathcal{R} = \mathcal{P}_n - (W_{t+\Delta t} - W_t) \quad (7)$$

[Figure 1 about here.]

Figure 1 shows that the subgrid scale variability of storage capacity allows the smallest local storage elements to saturate, and surface runoff to occur before the saturation of the whole soil. The soil moisture $W_{t+\Delta t}$ after net precipitation occurs can be decomposed into two terms : $S_{t+\Delta t}$, the soil moisture held in the saturated part of the soil and $N_{t+\Delta t}$, the soil moisture held in the unsaturated part of the soil. Let us detail the case of an initially dry soil ($W_t = 0$), illustrated in Figure 1. $S_{t+\Delta t}$ is given by the distribution function :

$$S_{t+\Delta t} = \int_0^{\mathcal{P}_n} c dF(c) = F(\mathcal{P}_n) \mathcal{P}_n - \int_0^{\mathcal{P}_n} F(c) dc \quad (8)$$

Since net precipitation is homogeneous through a grid-box, $N_{t+\Delta t}$ is given by

$$N_{t+\Delta t} = (1 - F(\mathcal{P}_n)) \mathcal{P}_n \quad (9)$$

where $(1 - F(\mathcal{P}_n))$ is the fraction of the grid-box in which the soil is not saturated. As a result of equations 8 and 9

$$W_{t+\Delta t} = S_{t+\Delta t} + N_{t+\Delta t} = \int_0^{\mathcal{P}_n} (1 - F(c)) dc \quad (10)$$

This result is generalized in Moore (1985), leading to the general form of surface runoff when the soil is not totally saturated :

$$\mathcal{R} = \mathcal{P}_n - (\bar{c} - W_t) + \bar{c} \left[\left(1 - \frac{W_t}{\bar{c}} \right)^{\frac{1}{b+1}} - \frac{\mathcal{P}_n}{(b+1)\bar{c}} \right]^{b+1} \quad (11)$$

When the whole soil is brought to saturation by the input of net precipitation, the surface runoff is the excess of water above maximum water content, and it is defined like the uniform surface runoff by

$$\mathcal{R} = \mathcal{P}_n - (\bar{c} - W_t) \quad (12)$$

Equations 11 and 12 define the SSV parameterization of surface runoff (SSV for Subgrid Scale Variability of storage capacity). This parameterization was originally designed to be used in specific catchments, as the Xinan-Jiang catchment (Zhao 1977), and the Arno catchment (Todini 1988). The SSV parameterization was also included in several soil hydrology parameterizations used in GCMs, like the Arno model (Dümenil and Todini 1992; Rowntree and Lean 1994) and the VIC model (Stamm et al. 1994), with values of b ranging between 0.01 and 0.5.

[Figure 2 about here.]

The response of surface runoff to the subgrid scale variability of storage capacity depends on the value of b , as it is illustrated in Figures 2a and 2b. They display the curves of $F(c)$ against c for different values of b , with \bar{c} always equal to 150 mm. In Figure 2a, c is normalized by c_{max} , which depends on b (equation 4). The uniform runoff is a special case of the SSV parameterization, when the shape parameter b is 0. It defines a constant storage capacity \bar{c} over the grid-box. In such a limiting case, the distribution function of storage capacity is a Dirac distribution. Figure 2a shows that small values of b define a small fraction of the grid-box fraction with small local storage capacities, and surface runoff is then close to the uniform surface runoff. On the contrary, the larger b is, the larger the grid-box fraction with small storage capacity, and more surface runoff is likely to happen. The limiting case of the distribution function F when $b \rightarrow +\infty$ is also interesting. Combining equations 3 and 4 gives

$$F(c^*) = 1 - \left(1 - \frac{c^*}{(b+1)\bar{c}}\right)^b \quad (13)$$

It follows, from the mathematical limit :

$$\lim_{x \rightarrow +\infty} \left(1 - \frac{a}{x}\right)^x = e^{-a} \quad (14)$$

that, when $b \rightarrow +\infty$

$$F(c^*) = 1 - e^{-c^*/\bar{c}} \quad (15)$$

This asymptotic exponential behavior is revealed in Figure 2b, where c is not normalized by c_{max} anymore. It is interesting because the exponential distribution is also used to account for subgrid scale processes in hydrology, especially for precipitation. It was used within the UKMO GCM (Warrilow et al. 1986), the GISS-II GCM (Johnson et al. 1993) and the CCM2 GCM (Bonan 1996).

3 Design of the GCM experiments

In the present study, the cycle 6 of the LMD GCM was used. The main features of this model are described in Sadourny and Laval (1984) and Le Treut and Li (1991), but this version includes the diurnal cycle (Polcher and Laval 1994) and the land surface scheme SECHIBA (Ducoudré et al. 1993). The only difference to the version presented in Polcher and Laval (1994) is the introduction of a new formulation for surface drag (Louis 1979). The GCM is run at the resolution of 64×50 , with grid-points regularly distributed in longitude and sine of latitude. This results in a resolution of about $5.6^\circ \times 2.4^\circ$ in the Tropics. Five simulations are conducted with this version of the LMD-GCM, forced with interannually varying sea surface temperatures (SST) from the AMIP dataset (Gates 1992) :

1. DRN : total runoff includes the uniform surface runoff of the reference version of SECHIBA (section 2.1) and the “two-speed” drainage parameterization (section 2.2). It is carried out for 10 years, with SST from 1979 to 1988.
2. TOT : DRN, with addition of the SSV parameterization of surface runoff, with the shape parameter $b=0.2$ in the range of Todini’s values (Dümenil and Todini 1992; Rowntree and Lean 1994) (10 years).
3. MIN : total runoff only includes the uniform surface runoff. This run is similar to DRN, minus the drainage parameterization (10 years).
4. TOT0.5 : as TOT, but the parameter b is changed to 0.5. It covers 4 years, and starts from the initial state of DRN at January 1st, 1981.
5. TOT5 : as TOT0.5, but $b=5$.

In these five simulations, the parameters of the studied hydrological parameterizations are constant all over the globe. For the comparison of the three 10-year simulations (MIN, DRN

and TOT), the first year was excluded, in order to reduce the effects of the initial conditions. It was checked on the remaining 9-year time series that there was no trend in the year to year variations of soil moisture. The analysis of the two 4-year simulations is performed over the four years.

4 Sensitivity to the SSV parameterization

In this section, we compare the simulations DRN and TOT, to study the sensitivity of the simulated hydrological cycle to the SSV parameterization, with $b=0.2$, and with drainage implemented.

Surface runoff strongly depends on net precipitation P_n (equation 6). In the GCM results presented here, the difference in moisture convergence (defined as the difference between total precipitation and total evaporation) between two simulations is a good approximation of the difference in net precipitation, because the snow and interception processes are very similar in all studied GCM simulations.

4.1 Global study

[Figure 3 about here.]

Figure 3a shows that, in January, surface runoff is greater in TOT than in DRN over most of the land areas. In the areas of small or negative moisture convergence (Figure 3b : the major part of the Northern Hemisphere continents), the SSV parameterization increases surface runoff compared to the control simulation DRN, but this increase is less than 0.1 mm/d. In the areas of higher moisture convergence (like the Inter Tropical Convergence Zone (ITCZ) or the mountains), the differences in surface runoff between DRN and TOT are larger, but they can be positive or negative. The high moisture convergence in these areas induces a frequent saturation of the soil. If the net precipitation is identical in both simulations, the surface runoff produced by the SSV parameterization is then identical to the uniform surface runoff in DRN (equation 12). The sign of the differences in surface runoff between DRN and TOT in high moisture convergence areas is therefore explained by the sign of the differences in moisture convergence (not shown). In contrast, the soil is rarely saturated in the areas of small moisture convergence and the uniform surface runoff is rare. The SSV parameterization achieves therefore

an increase of surface runoff from DRN to TOT even if the difference in monthly mean moisture convergence is negative.

The differences in surface runoff between the two simulations result from two distinct causes : the direct effects of the change in surface runoff parameterization and the feed-backs associated with the changes in moisture convergence. The daily surface runoff ratio is studied as a mean to extract the direct effects of the SSV parameterization on surface runoff. It is computed, in each grid-point and at a daily timestep, as the ratio of surface runoff to the exact net precipitation (equation 6), and is zero when the net precipitation is zero or negative. Figure 3c displays the January mean of the daily surface runoff ratio. It shows that, in January, the daily surface runoff ratio is greater in TOT than in DRN over almost all continental surfaces, with large areas where the increase of this ratio by the SSV parameterization is larger than 10%.

The same relations between surface runoff and moisture convergence are obtained for the other seasons. They are observed in particular in July, but the surface runoff increase with TOT in the extratropics is smaller because moisture convergence is smaller. Table 1 summarizes the differences between DRN and TOT over continents. It shows that the increase of annual mean surface runoff is very small, and not significant at the level $\alpha = 0.05$ with a student test. Soil moisture, evaporation and drainage decrease significantly from DRN to TOT. These significant changes can be related to the SSV parameterization because precipitation does not change significantly. On the opposite, total runoff (surface runoff + drainage) does not change significantly, because the variations of its two terms have opposite signs and similar magnitudes. The surface energy budget is very similar between DRN and TOT, as it appears for surface temperature in Table 1 (it is also true for its other components). This may be related to the fact that the changes in evaporation are very small.

[Table 1 about here.]

4.2 Regional study

To understand why the sensitivity of the LMD GCM to the subgrid scale variability of surface runoff is quantitatively so small, we focus our attention on two regions. The first one is the Mississippi basin, which covers 21 GCM grid-boxes, and displays in the LMD GCM a rather humid climate, with a large variability between the grid-boxes : the annual moisture convergence in DRN is 353 mm/year over the whole basin, and ranges from 0 to 2041 mm/year in the grid-

boxes. The second region is the Ob basin, in Siberia. The climate of this basin is characterized in the LMD GCM by a very weak moisture convergence (22 mm/year for the whole basin). For 9 of the 13 grid-boxes, the annual mean moisture convergence is lower than 10 mm/year.

[Figure 4 about here.]

In Figure 4, we compare the annual cycles of TOT and DRN, averaged over both basins. Student tests are performed to compare the monthly means of the two simulations. In the Mississippi basin, where precipitations are very similar in the two simulations, it is impossible to assess whether TOT produces significantly more surface runoff than DRN, except in December. In contrast, the daily surface runoff ratio is significantly higher with TOT, which indicates a direct effect of the SSV parameterization on surface runoff. Drainage is smaller in the simulation TOT over the entire year, and the difference is often significant. This decrease is explained by the decrease of soil moisture (not shown). The annual cycle of total runoff is not changed by the SSV parameterization, because its major component in the Mississippi basin is surface runoff, which does not change. In contrast with the Mississippi basin (Figure 4), the SSV parameterization strongly increases surface runoff in the Ob basin. This increase is all the more significant since precipitation is smaller in TOT than in DRN. The strong sensitivity of surface runoff to the SSV parameterization can also be seen in the daily surface runoff ratio, which is much more increased by the SSV parameterization in the Ob than in the Mississippi basin. Soil moisture is significantly decreased in the simulation TOT, from April to September, which induces a decrease of drainage. Soil moisture being small on average (33 mm compared to 68 mm in the Mississippi basin), drainage operates at low speed, and its decrease is not significant. The total runoff is significantly increased by the parameterization SSV, because surface runoff is increased in this dry basin, in contrast with the Mississippi basin.

4.3 Grid scale study

[Figure 5 about here.]

The annual water budgets in the two simulations are compared in every grid-box of the Mississippi basin, and the conclusions are similar to those obtained at the basin scale : the annual means of precipitation and moisture convergence are not statistically different in DRN and TOT in the Mississippi basin grid-boxes ; in most of them, the annual mean soil moisture is

decreased by the SSV parameterization, leading to a decrease of both evaporation and drainage, but the annual mean surface runoff is only slightly increased (Figure 5). The only grid-boxes where surface runoff is significantly higher in TOT than in DRN (grid-boxes 1,4,5,6 and also 2 and 3 at the level $\alpha = 0.10$) are the driest grid-boxes of the basin, where the soil does not reach saturation every winter. The SSV parameterization is designed to allow surface runoff to occur before soil saturation, when the uniform surface runoff does not operate, and it therefore slows down the filling of soil. If the climate is humid enough, the soil saturates sooner in DRN than in TOT, and there is a period during which DRN produces more surface runoff than TOT. This may counterbalance the increase of surface runoff by the SSV parameterization at drier periods. This suggests that the main effect of the SSV parameterization would be a spreading of the time distribution of surface runoff, and that the increase of the long term surface runoff average would be restricted to dry climates. Comparing the frequency distributions of surface runoff between TOT and DRN would then be expected to provide a better diagnostic of the real sensitivity to the SSV parameterization.

[Figure 6 about here.]

Frequency distributions of surface runoff (based on daily values) are presented in Figure 6. For the three studied grid-boxes, the distributions are different in DRN and TOT, and this can not be explained by differences in the frequency distributions of precipitation, which are very similar (not shown). The main difference is an increase of the frequency of the smallest surface runoff values in TOT. The uniform surface runoff included in DRN is a threshold process, and it displays a very large number of null surface runoff occurrences, when the soil is not saturated. With the SSV parameterization, they are replaced, when it is raining, by occurrences of small surface runoff. A major difference between the three grid-boxes studied in Figure 6 is their hydrological regime. In DRN, the annual mean moisture convergence is low in grid-box a (65 mm/year), it is higher in grid-box b (349 mm/year), and it is very high in grid-box c (2041 mm/year). The difference between TOT and DRN surface runoff frequency distributions decreases when the annual mean moisture convergence increases (Figure 6) : the higher the net precipitation, the longer the saturation, during which the surface runoff has the same characteristics whatever its parameterization.

[Figure 7 about here.]

The effect of the SSV parameterization on surface runoff frequency distribution and its modulation by the hydrological cycle are studied in each of the 21 grid-boxes of the Mississippi basin. Surface runoff values in both simulations are integrated over the same range of small surface runoff values $([0, lim])$, where the two distributions are clearly different. The difference is normalized in the coefficient C_{lim} :

$$C_{lim} = \frac{\left| \sum_0^{lim} r_{TOT} - \sum_0^{lim} r_{DRN} \right|}{\sum_0^{lim} r_{TOT}} \quad (16)$$

where r_{TOT} and r_{DRN} design the daily surface runoff values in TOT and DRN respectively. In the present study, $lim=4$ mm/d, which defines the largest range of surface runoff values in which the two frequency distributions are clearly different in the Mississippi basin.

Figure 7a plots C_4 against the annual mean moisture convergence in DRN. The high negative value of the correlation coefficient ρ confirms that the higher moisture convergence, the smaller the sensitivity to the SSV parameterization in a grid-box. This is confirmed in the Ob basin, where the surface runoff frequency distributions are strongly different between TOT and DRN in all grid-boxes. This is related to their small moisture convergence.

Student tests are performed for each grid-box of the Mississippi basin, to assess if the annual mean surface runoff is significantly different between TOT and DRN. The result of each test is given as a p-value, which gives the smallest possible value for the significance level. Under the assumptions of the tests, the p-value quantifies the risk of accepting that the two annual means are different. Figure 7b shows that it is easier to be sure that DRN and TOT have different annual mean surface runoff when the annual mean moisture convergence is small. In such a case, the annual mean surface runoff is small in DRN, and the increase in small surface runoff frequency by the SSV parameterization is able induce noticeable changes in mean surface runoff. Moreover, the comparison of Figures 7a and 7b confirms the validity of the coefficient C_{lim} as a measure of the sensitivity of surface runoff to the SSV parameterization.

4.4 Aggregation of grid-boxes

[Figure 8 about here.]

To understand why the annual cycles of surface runoff are so close for TOT and DRN at the basin scale (Figure 4), whereas surface runoff is sensitive to the SSV parameterization at the

grid scale, we study how surface runoff frequency distributions evolve as the basin grid-boxes are gradually aggregated together. The aggregation is performed by averaging the daily values of surface runoff, grid-box by grid-box.

Figure 8 displays the distributions at four stages of an aggregation. Figure 8a shows DRN and TOT surface runoff frequency distributions for the initial grid-box, which has a zero annual mean moisture convergence in DRN : there is a large difference between the two frequency distributions. Figure 8b compares surface runoff distributions when 8 grid-boxes are aggregated together : there remains a clear difference between the two simulations. On the contrary, in Figure 8c, when 15 grid-boxes are aggregated, the difference between the two frequency distributions decreases substantially, and it ends to disappear almost completely when the 21 grid-boxes of the basin are aggregated together. The uniform surface runoff can not occur before the soil is saturated. Because of the diversity of local climates, related to discrepancies in general circulation features, the periods during which the soil is saturated vary, both in starting date and length, between the grid-boxes. Aggregating the grid-boxes can therefore spread in time the spatial average of surface runoff, compared to the surface runoff of a single grid-box. Such an aggregation has a much smaller effect in TOT than in DRN because the SSV parameterization already spreads surface runoff in time. At a large scale, there is a similarity between the subgrid scale variability of storage capacities underlying the SSV parameterization, and the sub-basin scale variability of soil moistures among the grid-boxes, which is mainly driven by the atmosphere.

[Figure 9 about here.]

The coefficient C_4 is computed at each stage of the aggregation, and plotted against the number of grid-boxes aggregated at that stage. In Figure 9a, the aggregation is performed in the “order of increasing moisture convergence” (like in Figure 8) : the first grid-box has the smallest annual mean moisture convergence in DRN, and the last one has the highest. The opposite order is used in Figure 9b. These two orders represent the limiting cases for any aggregation in a random order. The two figures confirm that the aggregation decreases the differences between the two frequency distributions, and Figure 9b shows the importance of the wettest grid-boxes in that decrease. In these grid-boxes, the two surface runoff frequency distributions are hardly different, and the amount of surface runoff is very high (1639 mm/year for DRN for the wettest grid-box), which overrides the differences resulting from the dry grid-

boxes. The same study in the Ob basin confirms that the aggregation of very dry grid-boxes hardly decreases the difference in surface runoff frequency distribution at the grid scale.

5 Sensitivity to the drainage term

An result of the above section is that drainage is a highly sensitive hydrological variable, and that it has a noticeable impact on total runoff. In this section, we intend to assess the importance of the drainage term for the hydrological cycle, by comparing the simulations TOT and DRN, which include a drainage term, to the simulation MIN, with the uniform surface runoff and no drainage term.

5.1 Water budget and total runoff

Table 1 summarizes the differences between DRN, TOT and MIN over continents. In the latter simulation, drainage is not parameterized and the distinction between surface and total runoff is not relevant. Only total runoff is then compared between the three simulations.

Both drainage and the subgrid scale variability of surface runoff induce changes of the same sign in the annual average : they increase total runoff and decrease soil moisture and evaporation ; there is also a decrease of precipitation (not significant) as well as an increase of surface temperature. But with the parameters used for this study, drainage is more effective than the subgrid scale variability of surface runoff, as can be seen in the magnitude and the statistical significance of the differences in Table 1.

Those results can be compared with the study carried out by Stamm et al. (1994). They compared the VIC model to a bucket model in the GFDL GCM. The VIC model includes the subgrid scale variability of soil moisture capacity, with a shape parameter $b=0.3$ very close to the value we used ($b=0.2$). The VIC model also includes a drainage term : their choice of parameter implies a drainage of $3.10^{-2} \text{ mm.h}^{-1}$ for the maximum soil moisture (150 mm), which is close to our maximum drainage value of $5.10^{-2} \text{ mm.h}^{-1}$. For evaporation and precipitation, the changes induced by the VIC model are similar, both in magnitude and significance, to the changes between MIN and TOT in our experiment. But they found a total change of 13% for total runoff, and 25 mm for soil moisture, compared to 5% and 8 mm respectively in our experiment. We mainly ascribe the smaller variations in our experiment to an important

difference between the two drainage parameterizations : in the VIC model, drainage increases linearly with soil moisture, and it is efficient over a longer period than our non-linear “two-speed” drainage parameterization, in which drainage is negligible until soil moisture is 75% of its maximum value. The VIC model is especially efficient during the dry season, when it is able to increase total runoff by a large amount, as explained by Stamm et al. (1994) : “the VIC drainage term is the mechanism that provides this [total] runoff when the moisture-holding capacity is only partially filled”.

[Table 2 about here.]

[Figure 10 about here.]

Figure 10 compares the water budgets of the three simulations in 20 of the world largest river basins, which are a representative sample of the LMD GCM hydrological regimes. The full names of the rivers are listed in Table 2. There is no systematic increase of total runoff when the drainage or the subgrid scale variability of surface runoff is implemented. In particular, there is an unexpected decrease of total runoff from MIN to TOT in many tropical basins : in the Yangtze (Ya), Niger (Ni), Amazon (Az) and Orinoco (Or) basins, and to a certain extent in the Ganges (Ga) and Congo (Co) basins. Annual means of total runoff and moisture convergence are highly correlated, as a result of the long-term climatic balance of water fluxes, and the decrease of annual total runoff in the above listed tropical basins is explained by the decrease of annual mean moisture convergence. In contrast to total runoff, the evaporation rate systematically decreases from MIN to TOT, in relation to the decrease of soil moisture induced by both parameterizations. The decrease of annual mean moisture convergence in the above tropical basins can therefore not be explained in terms of water budgets, and should be related to atmospheric circulation changes.

5.2 Atmospheric water cycle

[Figure 11 about here.]

The aim of this section is to investigate the impact of the studied parameterizations on the atmospheric branch of the hydrological cycle. In the annual average, the increase of total runoff is related to an increase of moisture convergence over land, which is itself balanced by a decrease

of moisture convergence over the oceans, as depicted in Figure 11. The increase of the water vapor flux from the oceans towards the continents is especially clear in the tropics, where the Hadley-Walker circulation drives an important advection. A more detailed study is performed for the months of January and July.

5.2.1 January

[Figure 12 about here.]

[Figure 13 about here.]

Figure 12 displays the zonal means differences DRN-MIN and TOT-MIN, for evaporation, precipitation and moisture convergence in January over continents. The zonal means below 40°S are discarded, because they include less than three continental points, or the ice-cap in Antarctica. No change in the studied fluxes is found in the Northern Hemisphere, where the evaporation rate in winter depends rather on the radiative flux than on humidity. In contrast, there are differences of evaporation in the tropics, between MIN on one hand and DRN and TOT on the other hand. This confirms that, with the studied parameters, drainage has a larger effect than the SSV parameterization. To study the impact of the drainage parameterization, we compare MIN and DRN only. Figure 12 shows that, in the tropics, over continents, the introduction of drainage decreases evaporation and increases both precipitation and moisture convergence.

Figure 13 shows that the decrease of evaporation is a general feature in the continental tropics, whereas the changes of precipitation and moisture convergence are both positive and negative. The zonal increase of precipitation and moisture convergence appears mainly over Brazil and South-Eastern Africa. In January, these areas are within the ITCZ and undergo an intense convection. There, the increase of precipitation and moisture convergence due to drainage are statistically significant at the level $\alpha=0.05$, and they are much larger than the decrease of evaporation, which is indicative of the strong link between rainfall, convergence and circulation. Moreover, in some surrounding areas, moisture convergence displays a decrease, which is the enhancement of a divergence. The above changes seem related to the processes presented by Polcher (1995). This study showed that the decrease of evaporation due to tropical deforestation could induce an increase of precipitation in the tropics. It related this increase,

which was centered on the ITCZ, to an increase of sensible heat flux, which increased the frequency of deep convective events.

5.2.2 July

[Figure 14 about here.]

Figure 14a shows that, in July and at all latitudes, the introduction of drainage reduces evaporation, and the SSV parameterization reduces evaporation further. In the extratropics, the two parameterizations induce similar variations of evaporation. A reason may be that the SSV parameterization operates mainly in dry periods, when the soil moisture is low (section 4). The two parameterizations also induce a noticeable reduction of precipitation, whereas moisture convergence hardly changes. This suggests that the decrease of precipitation is related to the decrease of evaporation. We can infer that it is due to the recycling of evaporation, which is known to be an important source for precipitation in the intercontinental zones and especially in the extratropics in summer (Brubaker et al. 1993)

[Figure 15 about here.]

In the tropics, in contrast with January, the decrease of evaporation caused by drainage is not related to a clear increase of moisture convergence and precipitation. In particular, Figures 14b and 14c show an important decrease of both quantities between 10°N and 20°N. This anomaly is located in the Indian monsoon area.

Figure 15a shows the precipitation rate simulated over the monsoon area in July in simulation MIN. Compared to observed rainfall, the two zonal rainbelts, over the himalayan orography and around 15°N, are too pronounced, and the model fails in simulating the rainbelt over the North of India. According to Gadgil and Sajani (1997), the latter maximum, called the monsoon convergence zone, is of major importance to simulate the interannual variability of the monsoon rainfall over India. Figure 15b displays the precipitation field in July in DRN : higher values appear north of 20°N over India and South-East Asia. The difference between the two simulations (Figure 15c) shows a shift in precipitation from 15°N towards higher latitudes. This is related to a similar shift in moisture convergence between the two simulations, as well as to a weakening of the 850 hPa wind (about -2 m.s^{-1}) south of 15°N and its acceleration, with the same magnitude, between 15°N and 25°N. To assess whether the monsoon displacement

is significant in regard to the high interannual variability in the Indian monsoon area, the samples of nine July precipitation means in MIN and DRN are compared over the two boxes displayed in Figure 15c, using both the student t-test and the Wilcoxon rank-sum test (Polcher and Laval 1994). Both of these tests indicate that, at the level of significance $\alpha=0.05$, the mean precipitation is significantly smaller in DRN than in MIN over the southern box, and significantly higher in DRN than in MIN over the northern box. These results show that land-surface hydrology has an impact on the monsoon convergence zone.

6 Influence of the shape parameter b on the sensitivity to the SSV parameterization

The parameterization of drainage has been shown to induce much larger changes in the hydrological cycle than the SSV parameterization with the shape parameter $b=0.2$. It must be noticed that the sensitivity to the parameterization SSV was established in experiments with drainage. This sensitivity might be reduced by the inclusion of the drainage term, since the decrease of drainage caused by the SSV parameterization may reduce the decrease of soil moisture that could be expected as a direct effect of the SSV parameterization. We intend here to assess whether an increase of the shape parameter b is able to enhance the changes caused by the SSV parameterization. Two values of b are tested : the first one, $b=0.5$, lies in the range of values proposed by Todini (Dümenil and Todini 1992; Rowntree and Lean 1994), and the second one, $b=5$, should lead to a behavior close to the one of the asymptotic exponential distribution, as it appears in Figure 2.

6.1 Results

Simulations TOT0.5 and TOT5, corresponding to the values of the shape parameter $b=0.5$ and $b=5$ respectively, were carried out for four years, covering 1981-1984. For their comparison with MIN, DRN and TOT, we restricted the analysis of the latter simulations to the period 1981-1984. This makes the time series too short for a rigorous statistical study.

[Table 3 about here.]

Table 3 displays the annual continental water budget over four years for the five simulations under comparison. Two cases must be distinguished, according to whether drainage is parame-

terized or not. In the simulation MIN, where there is no explicit parameterization of drainage, the surface runoff has to balance moisture convergence on its own, and it is larger than in the simulations with drainage. In these experiments, surface runoff increases as b increases from small values (DRN with $b=0$, TOT and TOT0.5) to the high value $b=5$ (TOT5). The increase of surface runoff is larger than the decrease of drainage, and total runoff increases from DRN to TOT5. This increase has the same magnitude as between MIN and DRN. As previously explained, the gradual increase of total runoff from MIN to TOT5 decreases soil moisture and evaporation, and it increases continental moisture convergence. Because of the short period of analysis, it is difficult to determine if the small precipitation decrease is due to the changes in the hydrological parameterizations, or if it is an effect of the inner variability of the GCM.

[Figure 16 about here.]

Figure 16 shows the mean annual cycles of the variables describing soil hydrology, as obtained for the Mississippi basin in the simulations with drainage (DRN, TOT, TOT0.5 and TOT5). Because of the short period of analysis, we excluded three of the wettest grid-boxes (located in the Rocky Mountains) to maximize the differences between the simulated surface runoffs, according to the results of section 4.4 (this does nevertheless not change the general shape of surface runoff annual cycles). Figure 16 shows a strong increase of surface runoff from DRN to TOT5. It is noticeable that the SSV parameterization operates mainly when the soil moisture is not too high : comparing DRN with TOT and TOT0.5, the largest differences in surface runoff occur from October to January, when the soil is filling and the soil moisture is lower than 80 mm. In TOT5, the monthly mean soil moisture is below 80 mm over the entire year, and the surface runoff is higher than in the other simulations. In summer, all simulations produce very little surface runoff because the soil moisture is very low and the net precipitation frequently negative. In contrast, drainage operates only when soil moisture is high (in winter and spring here), because of its “two-speed” parameterization. This explains why drainage is so weak in TOT5, since soil moisture is rather low in this simulation, being certainly below the threshold soil moisture (section 2.2) during the major part of winter and spring. Figure 16 shows that the total runoff is mainly increased during the replenishment period. The magnitude of this increase depends on b , because it is driven by the increase of surface runoff by the SSV parameterization. In the period of highest soil moisture (typically March), total runoff is similar in all simulations,

because drainage is no more negligible, and its decrease can balance the increase of surface runoff. This is especially clear in TOT5.

[Figure 17 about here.]

In spite of operating at different ranges of soil moisture, the two parameterizations share the ability to increase total runoff and continental moisture convergence. Figure 17 confirms that the SSV parameterization with $b=5$ enhances the evaporation decrease induced by drainage, and this enhances the precipitation decrease in the extratropics. Figure 11 (section 5) shows that, on the nine-year average, the continental moisture convergence increases from MIN to DRN. Such an increase is not as important on the four-year average in Figure 17. This may be related to the short period of analysis, and also to the fact that this period includes a very strong El Niño event (1982-83), which may increase the variability of the hydrological cycle. Nevertheless, Figure 17 indicates that the SSV parameterization with $b=5$ strengthens the increase of continental moisture convergence initiated by drainage. In the tropics, the SSV parameterization with $b=5$ could not be related to any significant change in precipitation neither in zonal mean (Figure 17) nor at a regional scale. This might be due to the short length of simulation TOT5.

The above study confirms that the increase of b increases the global effect of the SSV parameterization, but the clearest sensitivity is found in the extratropics on the basis of a four-year analysis. Johnson et al. (1993) tested the parameterization of land-surface hydrology of Entekhabi and Eagleson (1989) in the GISS-II GCM. This parameterization includes a subgrid scale variability of rainfall, which is inversely related, by an exponential law, to a fractional wetting coefficient κ . Surface runoff depends on the heterogeneity of soil properties according to a gamma distribution. It depends also on precipitation intensity, because the local surface runoff occurs when the local precipitation intensity exceeds the saturated soil hydraulic conductivity. No drainage is parameterized, and the total runoff equals the surface runoff. This land-surface parameterization had a large impact on the climate of the GISS-II GCM. The changes were mainly located in the tropics, and consisted in a strong increase of total runoff (it could be doubled) and in a strong decrease of evaporation. Precipitation was reduced, but to a lesser extent. It may be inferred that the mechanism inducing the largest changes is the subgrid scale variability of precipitation, because the fractional wetting coefficient κ had to be reduced substantially (from 0.6 to 0.15) to achieve the large changes summarized above. These changes with

$\kappa=0.15$ were much larger than ours, even between MIN and TOT5. This may be related to the dependence of their surface runoff on precipitation intensity : for the same precipitation amount, their surface runoff is larger if precipitation falls all of a sudden than if it is distributed over a long period. Such a mechanism is not at all simulated in our hydrological parameterization.

6.2 Comparison with observed data

[Table 4 about here.]

Table 4 presents estimates of the world water balance from different recent sources. There is a wide confidence band on these estimates (Henning 1989), because of the insufficient spatial sampling of observed data, the biases in the measurements and the assumptions of the assimilation methods. As an example of the large confidence range in such estimates, Legates and Willmott (1990) give two very different estimates of continental precipitation : 754 mm/year without adjustment for gage measurement biases, and 820 mm/year when this adjustment is done. The comparison of Table 4 with Tables 1 and 3 shows a large overestimation of continental precipitation in all studied simulations. The origin of this systematic overestimation may be the overestimation of oceanic moisture divergence in the GCM : over the oceans, the precipitation ranges between 1014 and 1030 mm/year according to the simulation, and the evaporation does not change (1238 mm/year) : this results in an overestimation of oceanic divergence by about 100 mm/year. The systematic overestimation of continental precipitation results in a systematic overestimation of continental evaporation and total runoff. This makes very difficult to assess which hydrological parameterization gives the most sensible total runoff. The strong relation of the total runoff overestimation to the precipitation overestimation is also revealed at the basin scale. We compared, over the basins listed in Table 2, the simulated annual total runoffs to observed per unit area annual river discharges (Russel and Miller 1990; GRDC 1994), and the simulated annual precipitation to the estimates of Russel and Miller (1990). This shows that the total runoff is underestimated where the precipitation is underestimated (for instance over the Amazon, the Orinoco and the Ob basins), and that it is conversely overestimated where the precipitation is overestimated. The difference between the simulated total runoffs is generally much smaller than the error compared to observations.

[Figure 18 about here.]

Figure 18 displays the simulated (DRN and TOT5) and observed (Wallis et al. 1991) annual cycles of total runoff and precipitation over the Mississippi basin. The observed total runoffs are approximated by the ratio of observed streamflows to the contributing areas in the stream gauging stations. On the monthly basis, it is a sensible estimate of total runoff at the GCM grid scale, because of the many gauging stations in the Mississippi basin, chosen to be as free as possible from the effects of water management (Wallis et al. 1991). As for Figure 16, we excluded three grid-boxes of the Rocky Mountains from the basin average. Only a fraction of these grid-boxes lies in the real catchment, and the GCM precipitation is strongly overestimated in the Rocky Mountains : the exclusion of the three grid-boxes improves the simulated annual mean precipitation over the basin. Figure 18 shows that the SSV parameterization with $b=5$ improves the annual cycle of total runoff, by increasing it from October to January, during the replenishment period. Such an improvement is initiated with smaller values of b (Figure 16). Total runoff remains poorly simulated from May to September, due to the underestimation of precipitation at this period.

7 Conclusion

The aim of this paper was to assess the sensitivity of the simulated climate, and particularly of the hydrological cycle, to different hydrological parameterizations. We tested in GCM simulations the impact of

- introducing a “two-speed” drainage parameterization,
- replacing the uniform surface runoff by a surface runoff accounting for the subgrid scale variability of soil water storage capacity (through the SSV parameterization).

The drainage parameterization is shown to have a significant impact on the hydrological cycle : it increases total runoff and decreases soil moisture and evaporation. The SSV parameterization is shown to modify the time distribution of surface runoff during the year, mainly by increasing the frequency of small surface runoff values. The average effect of the SSV parameterization on surface runoff is shown to depend on two factors. The first one is the hydrological regime : the surface runoff increase caused by the SSV parameterization is much larger when the soil moisture is low, and therefore when the annual mean moisture convergence is not too high.

The second factor influencing the response of surface runoff to the SSV parameterization is the value of the shape parameter b of the distribution function. In our GCM experiments, it has been necessary to strongly increase b to get a surface runoff increase able to cause a substantial increase in total runoff. With such a high value ($b=5$, compared to the first tested value $b=0.2$), the total runoff increase, as well as the soil moisture and evaporation decreases, have the same magnitude as the changes induced by the parameterization of drainage.

These two parameterizations induce similar changes in the atmospheric branch of the hydrological cycle. In the extratropics, they mainly consist in a reduction of precipitation in summer, by means of the recycling of evaporation into precipitation. In the tropics, the annual mean moisture convergence increases over land and decreases over oceans. The continental mean precipitation is not markedly changed, but seasonal studies pointed out that precipitation is sensitive to the hydrological parameterizations within the ITCZ and monsoon areas.

In spite of similarities between the global effects of the two parameterizations, there remains important differences in their time properties. The SSV parameterization operates when the soil is rather dry, in contrast with drainage, which operates when the soil is wet. The studied two parameterizations have also a different impact on the characteristic timescale of total runoff. Drainage has a long characteristic timescale because it strongly depends on soil moisture, and the characteristic timescale of surface runoff is shorter because it depends on net precipitation. By increasing surface runoff frequency, the parameterization SSV decreases the characteristic timescale of surface runoff (Polcher et al. 1996). The increase of b lessens the influence of soil moisture on surface runoff (equation 11), and it therefore increases the relative power of high frequencies related to net precipitation, to the detriment of the low frequencies related to soil moisture. An important issue will therefore be to assess the importance for GCMs of the differences in total runoff characteristic timescale related to the above two processes. The phasing and characteristic timescale of the total runoff are important for climatological studies because they influence the time evolution of soil moisture and evaporation, and therefore the whole hydrological cycle. This is an important issue for the coupling of atmospheric and oceanic GCMs too, because of the influence of fresh water for ocean salinity, and the dynamics of oceans and sea-ice. In the framework of climate change, it is also of major concern to have a proper estimate of the annual cycle of river discharge, because of the importance of floods in water management. The comparison of simulated and observed total runoff in the Mississippi basin

shows that the soil hydrological parameterizations have the ability to improve the annual cycle of total runoff. Generalizing this result will need as a prerequisite to improve annual mean precipitation, which strongly influences annual mean total runoff.

An important issue raised by the present study addresses the value of the shape parameter b for use in GCMs. Dümenil and Todini (1992) state that a typical average value for b in a single catchment as the Arno catchment is $b=0.2$, and in the ECHAM2 GCM, b varies between 0.01 and 0.5, as a function of the subgrid variability of orography. The parameter b was calibrated on several single catchments : on the French Broad River catchment in North Carolina, with precipitation and temperature data from a nearby meteorological station, Wood et al. (1992) found $b=0.085$ and $b=0.129$, depending on the assumed average storage capacity over the catchment ; Liang et al. (1994) found $b=0.008$ on the King's Creek catchment in Kansas, with meteorological inputs from the FIFE site (Sellers et al. 1992). Sivapalan et Woods (1995) estimated the value of $b=4.03$ directly from field data on the Serpentine catchment in Australia. At a larger scale, Stamm et al. (1994) estimated the global distribution of b for use in the GFDL GCM at R15 resolution from a $0.5^\circ \times 0.5^\circ$ data set of water storage capacity (Patterson 1990). They found values ranging from 0 to 7.9, with a mean global value of $b=1.2$. The above values display a wide variability whatever the spatial scale under consideration, and following Entekhabi and Eagleson (1989), we infer that "the magnitude of the coefficient of variation of soil moisture content increases with the size of the field due to increased heterogeneity of topography and geology at larger scales". Such an assumption is coherent with the results by Johnson et al. (1993), who improved the simulated water cycle in the GISS-II GCM by reducing the fractional wetting coefficient of their subgrid land-hydrology parameterization (section 6.1) to match the coarse resolution of the GCM. An extensive work on the spatial distribution of soil properties at various scales would allow to assess the above assumption. Whatever the result, it is thought to be a necessary step toward a better modeling of land-surface hydrology in GCMs, because of the strong sensitivity exhibited by the LMD GCM to the shape parameter b .

Acknowledgments

We are very grateful to Bryan Weare and the two referees for their fruitful comments, which helped to improve the manuscript. We thank Lydia Dümenil and the Max-Planck-Institut für Meteorologie for providing us with the SSV and drainage parameterizations. We also thank the

Global Runoff Data Center for the observed river discharge data, Dennis P. Lettenmaier for the observed data over the Mississippi basin, and the Institut du Développement et des Ressources en Informatique Scientifique for the computational support.

References

- Baumgartner, A., and E. Reichel, 1975: *The World Water Balance*. Elsevier.
- Bergström, S., and A. Forsman, 1973: Development of a conceptual deterministic rainfall-runoff model. *Nordic Hydrology*, **4**,147–170.
- Bonan, G. B., 1996: Sensitivity of a GCM simulation to subgrid infiltration and surface runoff. *Climate Dynamics*, **12**,279–285.
- Brubaker, K. L., D. Entekhabi, and P. S. Eagleson, 1993: Estimation of continental precipitation recycling. *J Climate*, **6**,1077–1089.
- Budyko, M. I., 1978: The heat balance of the Earth. *Climatic change*, J. Gribbin, Ed., pp. 85–113. Cambridge University Press.
- Choisnel, E. M., S. V. Jourdain, and C. J. Jacquart, 1995: Climatological evaluation of some fluxes of the surface energy and soil water balances over France. *Annales Geophysicae*, **13**,666–674.
- Dickinson, R. E., 1984: Modeling evaporation for three-dimensional global climate models. *Climate Processes and Climate Sensitivity, Volume 5*, pp. 58–72.
- Ducoudré, N., K. Laval, and A. Perrier, 1993: SECHIBA, a new set of parametrizations of the hydrologic exchanges at the land/atmosphere interface within the LMD atmospheric general circulation model. *J Climate*, **6**,248–273.
- Dümenil, L., and E. Todini, 1992: A rainfall-runoff scheme for use in the Hamburg climate model. *Advances in theoretical hydrology, A tribute to James Dooge*, V. 1 of *European Geophysical Society Series in Hydrological Sciences*, J. O’Kane, Ed., pp. 129–157. Elsevier.
- Entekhabi, D., and P. Eagleson, 1989: Land surface parametrization for atmospheric general circulation models including subgrid scale spatial variability. *J Climate*, **2**,32–46.

- Gadgil, S., S. Sajani, and Participating Modelling Groups of AMIP, 1997: Monsoon precipitation in the AMIP runs. Draft Report of Results from an AMIP Diagnostic Subproject, submitted to Climate Dynamics.
- Gates, W. L., 1992: AMIP, the Atmospheric Model Intercomparison project. *Bulletin of the American Meteorological Society*, **73**,1962–1970.
- GRDC, 1994: Hydrological regimes of the 20 largest rivers of the world - A compilation of the GRDC database. Technical Report 5, Global Runoff Data Center, Koblenz, Germany.
- Henning, D., 1989: *Atlas of the Surface Heat Balance of the Continents*. Gebrüder Borntraeger, Berlin.
- Johnson, K. D., D. Entekhabi, and P. S. Eagleson, 1993: The implementation and validation of improved land-surface hydrology in an atmospheric general circulation model. *J Climate*, **6**,1009–1026.
- Koster, R. D., and M. J. Suarez, 1992: Modeling the land surface boundary in climate models as a composite of independent vegetation stands. *J Geophys Res*, **97**,2697–2715.
- Laval, K., C. Ottle, A. Perrier, and Y. Serafini, 1984: Effect of parametrisation of evapotranspiration on climate simulated by a GCM. *New perspectives in climate modelling*, A. L. Berger, and C. Nicolis, Eds., pp. 223–247. Elsevier Science Publishers, Amsterdam.
- Le Treut, H., and Z.-X. Li, 1991: Sensitivity of an atmospheric general circulation model to prescribed SST changes: feedback effects associated with the simulation of cloud optical properties. *Clim Dyn*, **5**,175–187.
- Legates, D. R., and C. J. Willmott, 1990: Mean seasonal and spatial variability in gauge-corrected, global precipitation. *International Journal of Climatology*, **10**,111–127.
- Liang, X., D. P. Lettenmaier, E. F. Wood, and S. J. Burges, 1994: A simple hydrologically based model of land surface water and energy fluxes for general circulation models. *J Geophys Res*, **99**,14,415–14,428.
- Louis, J. F., 1979: A parametric model of vertical eddy fluxes in the atmosphere. *Bound Layer Meteor*, **17**,187–202.

- Manabe, S., 1969: Climate and the ocean circulation 1. The atmospheric circulation and the hydrology of the earth's surface. *Mon. Weather. Rev.*, **97**,739–774.
- Milly, P. C. D., 1992: Potential evaporation and soil moisture in general circulation models. *J Climate*, **5**,209–226.
- Milly, P. C. D., and K. A. Dunne, 1994: Sensitivity of the global water cycle to the water-holding capacity of land. *J Climate*, **7**,506–526.
- Moore, R. J., 1985: The probability-distributed principle and runoff production at point and basin scales. *Hydrological Sciences*, **30**,273–297.
- Patterson, K. A., 1990: Global distributions of total and total-available soil water holding capacities. Master's thesis, University of Delaware.
- Polcher, J., 1995: Sensitivity of tropical convection to land surface processes. *J Atmos Sci*, **52**,3143–3161.
- Polcher, J., and K. Laval, 1994: A statistical study of regional impact of deforestation on climate of the LMD-GCM. *Clim Dyn*, **10**,205–219.
- Polcher, J., K. Laval, L. Dumenil, J. Lean, and P. R. Rowntree, 1996: Comparing three land surface schemes used in general circulation models. *J Hydrol*, **180**,373–394.
- Rowntree, P. R., and J. Lean, 1994: Validation of hydrological schemes for climate models against catchment data. *J Hydrol*, **155**,301–323.
- Russel, G. L., and J. R. Miller, 1990: Global river runoff calculated from a global atmospheric general circulation model. *J Hydrol*, **117**,241–254.
- Sadourny, R., and K. Laval, 1984: January and July performance of the LMD general circulation model. *New perspectives in climate modelling*, A. L. Berger, and C. Nicolis, Eds., pp. 173–197. Elsevier Science Publisher, Amsterdam.
- Sellers, P., Y. Mintz, Y. Sud, and A. Dachler, 1986: A simple biosphere model (SiB) for use within general circulation models. *J Atmos Sci*, **46**,505–531.

- Sellers, P. J., F. G. Hall, A. G., D. E. Strebel, and R. E. Murphy, 1992: A overview of the First International Satellite Land Surface Climatology Project (ISLSCP) field experiment. *J Geophys Res*, **97** (D17), 18345–18371.
- Sivapalan, M., and R. A. Woods, 1995: Evaluation of the effects of general circulation model's subgrid variability and patchiness of rainfall and soil moisture on land surface water balance fluxes. *Hydrological Processes*, **9**, 697–717.
- Stamm, J. F., E. F. Wood, and D. P. Lettenmaier, 1994: Sensitivity of a GCM simulation of global climate to the representation of land-surface hydrology. *J Climate*, **7**, 1218–1239.
- Todini, E., 1988: Il modello afflussi deflussi del fiume Arno. Relazione Generale dello studio per conto della Regione Toscana, University of Bologna.
- Wallis, J. R., D. P. Lettenmaier, and E. F. Wood, 1991: A daily hydroclimatological data set for the continental United States. *Water Resources Research*, **27**, 1657–1663.
- Warrilow, D. A., A. B. Sangster, and A. Slingo, 1986: Modelling of land surface processes and their influence on European climate. Dynamical Climatology DCTN38, Meteorological Office, Bracknell, UK.
- Wood, E., D. Lettenmaier, and V. Zartarian, 1992: A land-surface hydrology parameterization with subgrid variability for general circulation models. *J Geophys Res*, **97**, 2717–2728.
- Zhao, R., 1977: *Flood forecasting method for humid regions of China*. East China College of Hydraulic Engineering, Nanjing, China.

List of Figures

1	Schematic of surface runoff production with a subgrid scale variability of water storage capacity (case of an initially dry soil : $W_t = 0$). The curve plots c against $F(c)$, and represents the maxima of the local water contents.	31
2	F as a function of a normalized soil water content and b soil water content c for different values of the shape parameter b	32
3	January monthly means : a surface runoff difference (TOT-DRN) in mm/d, b moisture convergence in DRN in mm/d, c daily surface runoff ratio difference (TOT-DRN).	33
4	The Mississippi and Ob basins : mean annual cycles (monthly values) of surface runoff, daily surface runoff ratio and drainage. A star indicates that the monthly means of DRN and TOT are significantly different at the level $\alpha = 0.05$	34
5	The Mississippi basin : differences (TOT - DRN) in the annual mean surface runoff in every grid-box of the basin. Bars in dark grey indicate a significant difference at the level $\alpha = 0.05$. The grid-boxes are numbered from the smallest to the largest annual mean moisture convergence in DRN.	35
6	The Mississippi basin : frequency distributions of surface runoff (DRN and TOT) in three grid-boxes. Their annual mean moisture convergence in DRN increases from a to c	36
7	For each grid-box of the Mississippi basin : a coefficient C_4 for surface runoff against annual mean moisture convergence in DRN, b p-value of the student test comparing the annual mean surface runoff in TOT and DRN against the annual mean moisture convergence in DRN. A linear regression is drawn through the points, and ρ is the correlation coefficient.	37
8	The Mississippi basin : frequency distributions of surface runoff for DRN and TOT : a one grid-box, b aggregation of 8 grid-boxes, c aggregation of 15 grid-boxes, d aggregation over the whole basin.	38
9	The Mississippi basin : coefficient C_4 for surface runoff against the number of aggregated grid-boxes ; aggregation following the order of a increasing, b decreasing, annual mean moisture convergence in DRN. A linear regression is drawn through the points, and ρ is the correlation coefficient.	39
10	Comparison of DRN, TOT and MIN over 20 of the world largest river basins : annual means (per unit area, in m/year) of a total runoff and b evaporation. . .	40
11	Year : zonal mean of the difference (DRN - MIN) in moisture convergence (mm/d) over land and oceans.	41
12	January : zonal means over land of the differences DRN-MIN and TOT-MIN (mm/d), in a evaporation, b precipitation and c moisture convergence.	42
13	January : differences (DRN - MIN) in mm/d for a evaporation : contours at -0.6, -0.3, 0, 0.3, 0.6 ; b precipitation and c moisture convergence : contours at -2, -1, -0.5, 0.5, 1, 2.	43
14	July : zonal means over land of the differences DRN-MIN and TOT-MIN (mm/d), in a evaporation, b precipitation and c moisture convergence.	44
15	July : precipitation (mm/d) a in MIN and b in DRN ; contours at 2, 5, 10, 15, 20 , c difference (DRN-MIN) ; contours at -4, -2, -1, 1, 2, 4.	45

16	The Mississippi basin : mean annual cycles (monthly values, mm/d) simulated by DRN, TOT, TOT0.5 and TOT5, for surface runoff, drainage, total runoff and soil moisture. The time axis ranges from October to September.	46
17	Annual zonal means over land of the differences DRN-MIN and TOT5-MIN, for a evaporation, b precipitation and c moisture convergence.	47
18	The Mississippi basin : comparison of simulated (DRN and TOT5) annual cycles of total runoff and precipitation with observed data (Wallis et al. 1991).	48

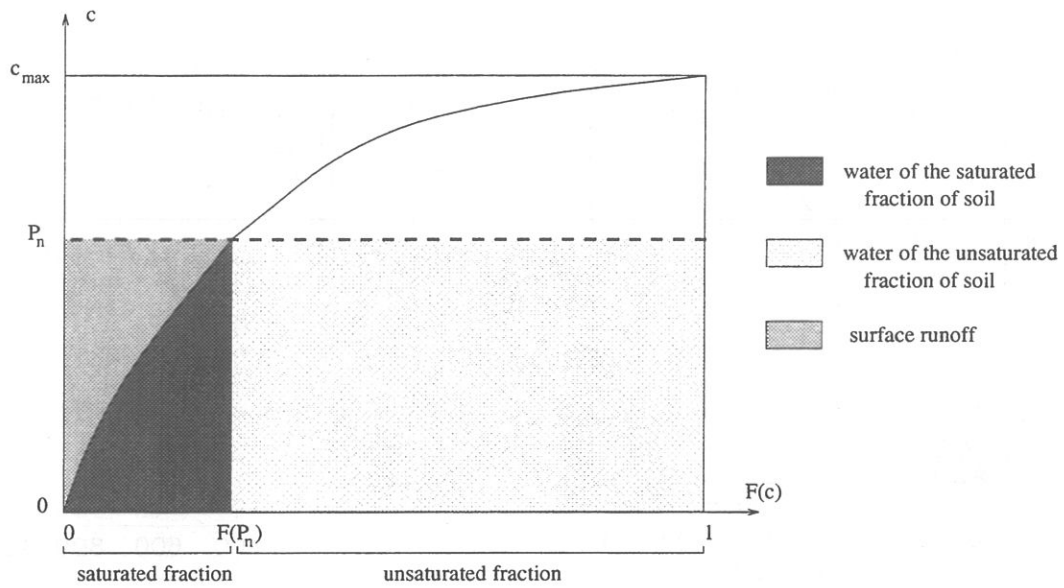


Figure 1: Schematic of surface runoff production with a subgrid scale variability of water storage capacity (case of an initially dry soil : $W_t = 0$). The curve plots c against $F(c)$, and represents the maxima of the local water contents.

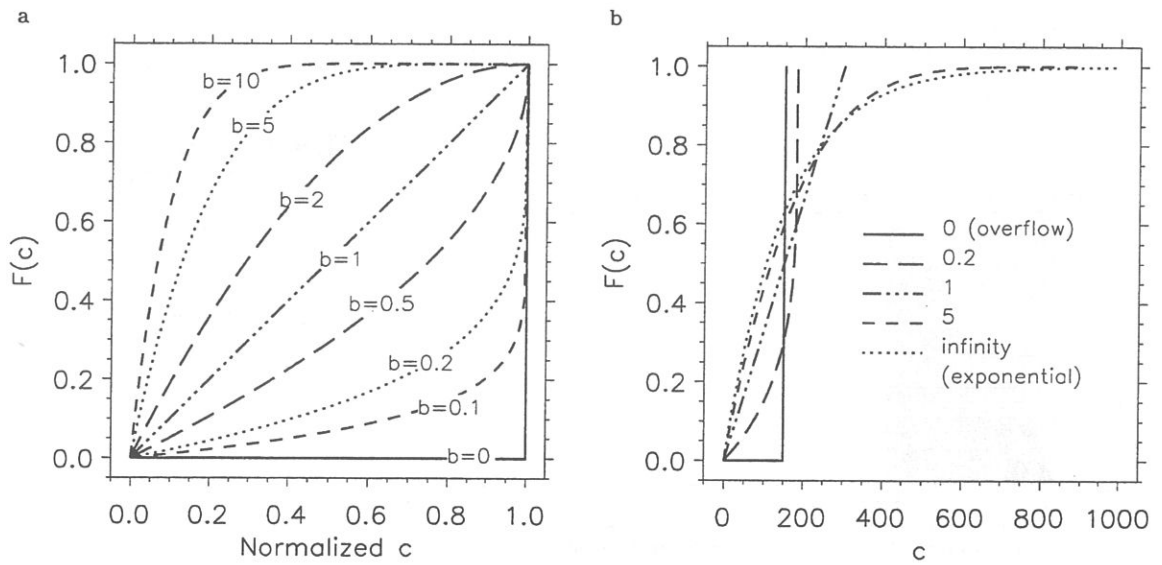


Figure 2: F as a function of **a** normalized soil water content and **b** soil water content c for different values of the shape parameter b .

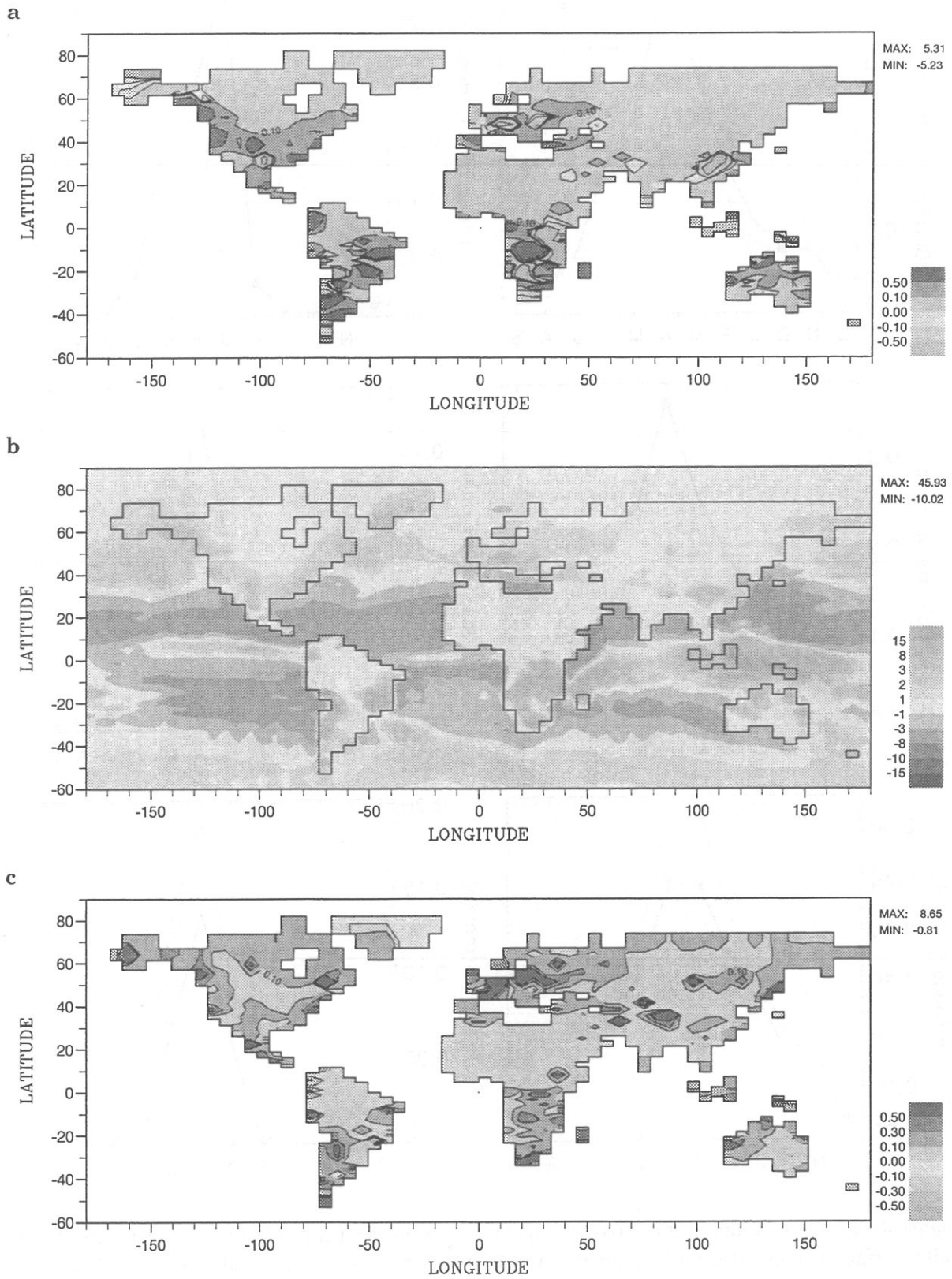


Figure 3: January monthly means : **a** surface runoff difference (TOT-DRN) in mm/d, **b** moisture convergence in DRN in mm/d, **c** daily surface runoff ratio difference (TOT-DRN).

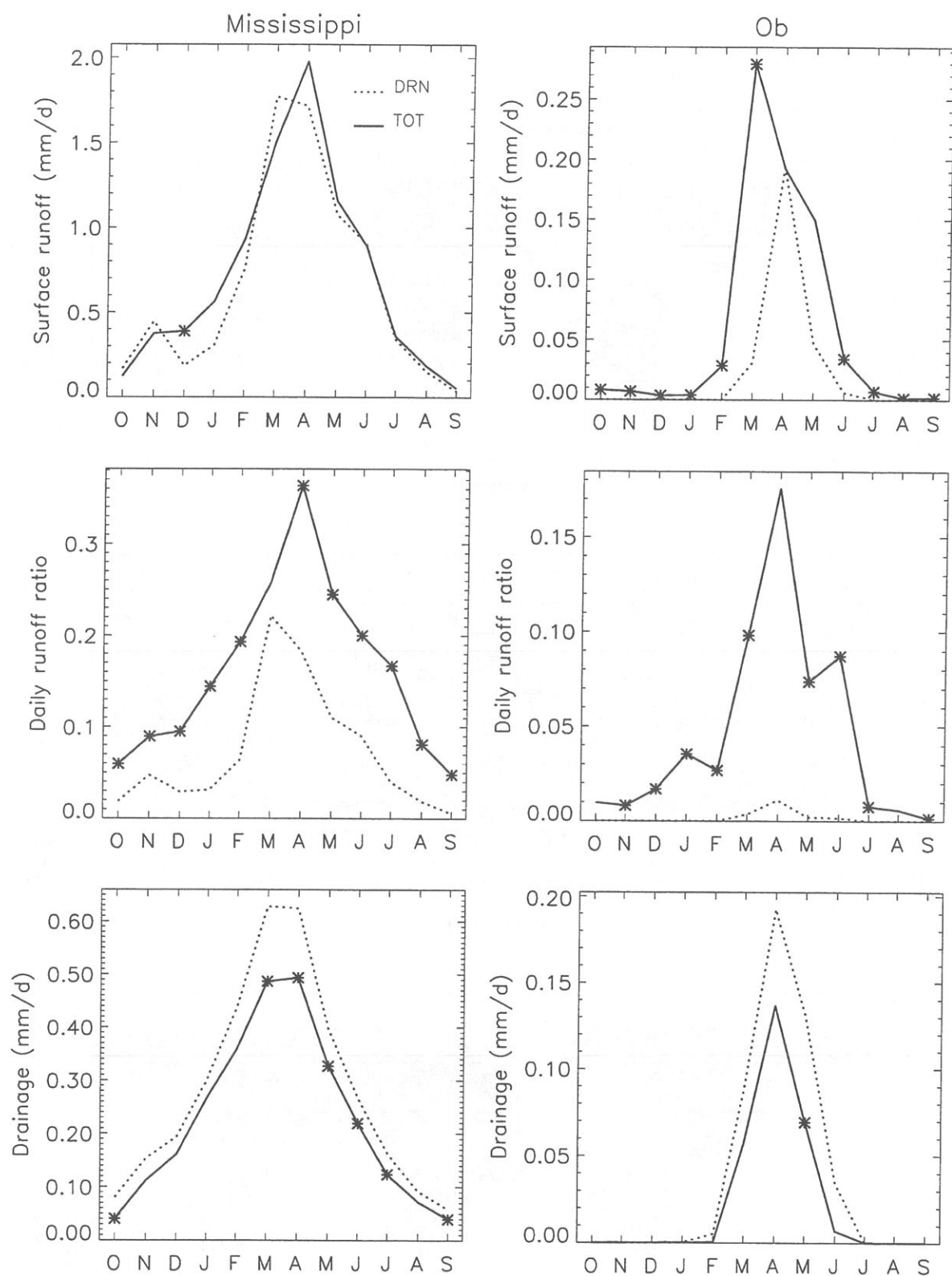


Figure 4: The Mississippi and Ob basins : mean annual cycles (monthly values) of surface runoff, daily surface runoff ratio and drainage. A star indicates that the monthly means of DRN and TOT are significantly different at the level $\alpha = 0.05$.

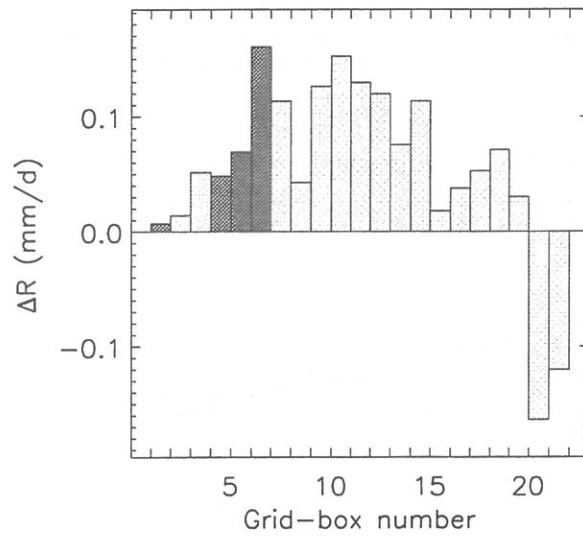
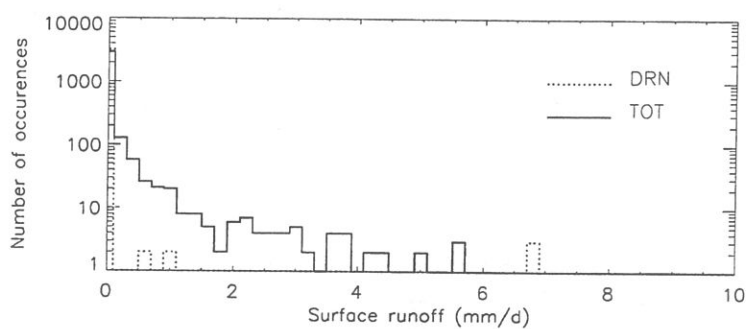
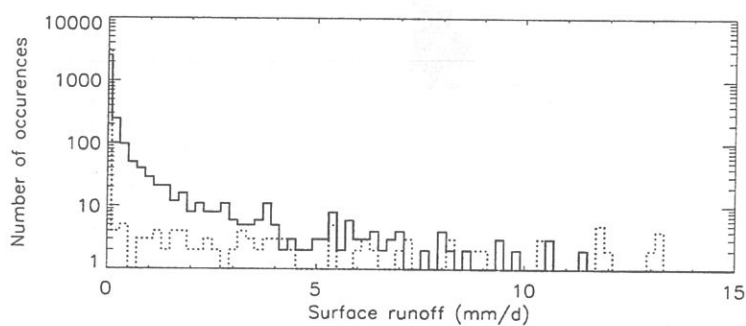


Figure 5: The Mississippi basin : differences (TOT - DRN) in the annual mean surface runoff in every grid-box of the basin. Bars in dark grey indicate a significant difference at the level $\alpha = 0.05$. The grid-boxes are numbered from the smallest to the largest annual mean moisture convergence in DRN.

a



b



c

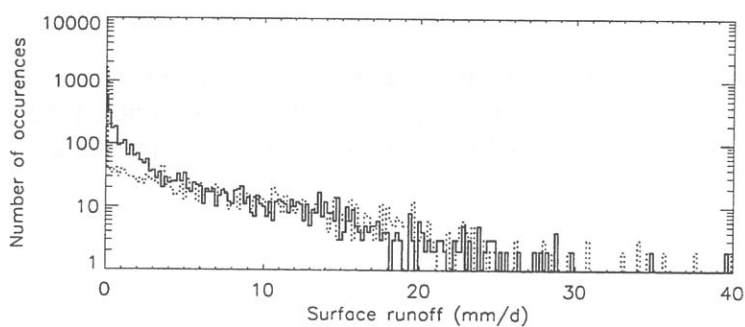


Figure 6: The Mississippi basin : frequency distributions of surface runoff (DRN and TOT) in three grid-boxes. Their annual mean moisture convergence in DRN increases from **a** to **c**.

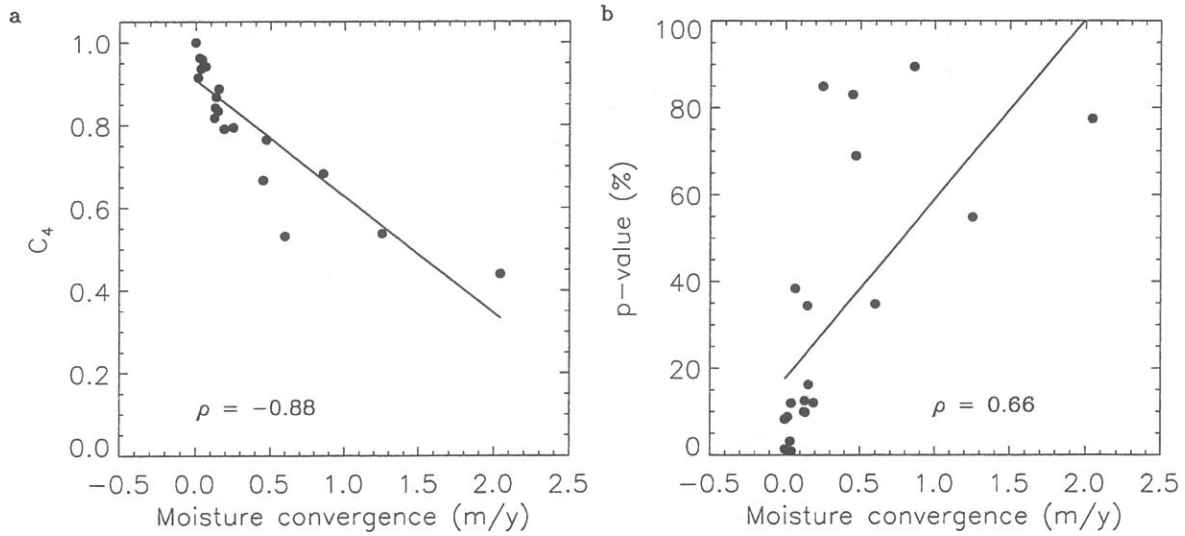
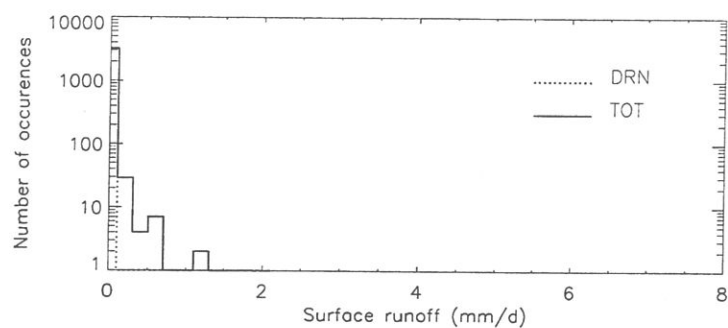
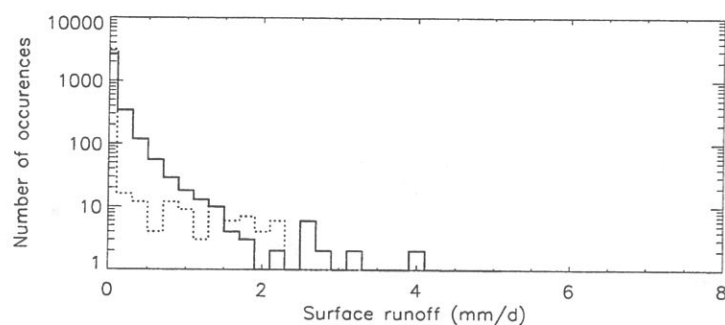


Figure 7: For each grid-box of the Mississippi basin : **a** coefficient C_4 for surface runoff against annual mean moisture convergence in DRN, **b** p-value of the student test comparing the annual mean surface runoff in TOT and DRN against the annual mean moisture convergence in DRN. A linear regression is drawn through the points, and ρ is the correlation coefficient.

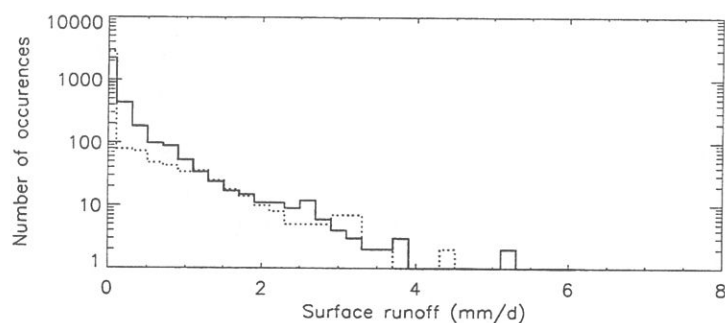
a



b



c



d

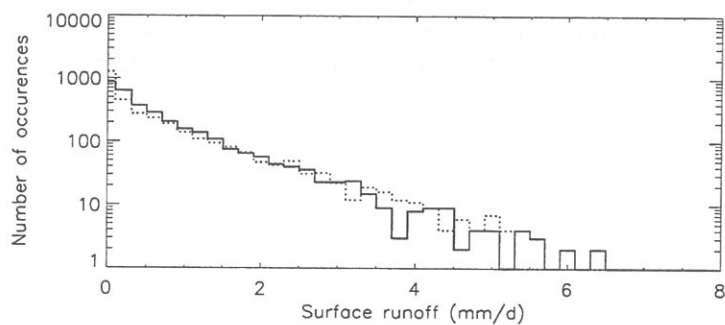


Figure 8: The Mississippi basin : frequency distributions of surface runoff for DRN and TOT : **a** one grid-box, **b** aggregation of 8 grid-boxes, **c** aggregation of 15 grid-boxes, **d** aggregation over the whole basin.

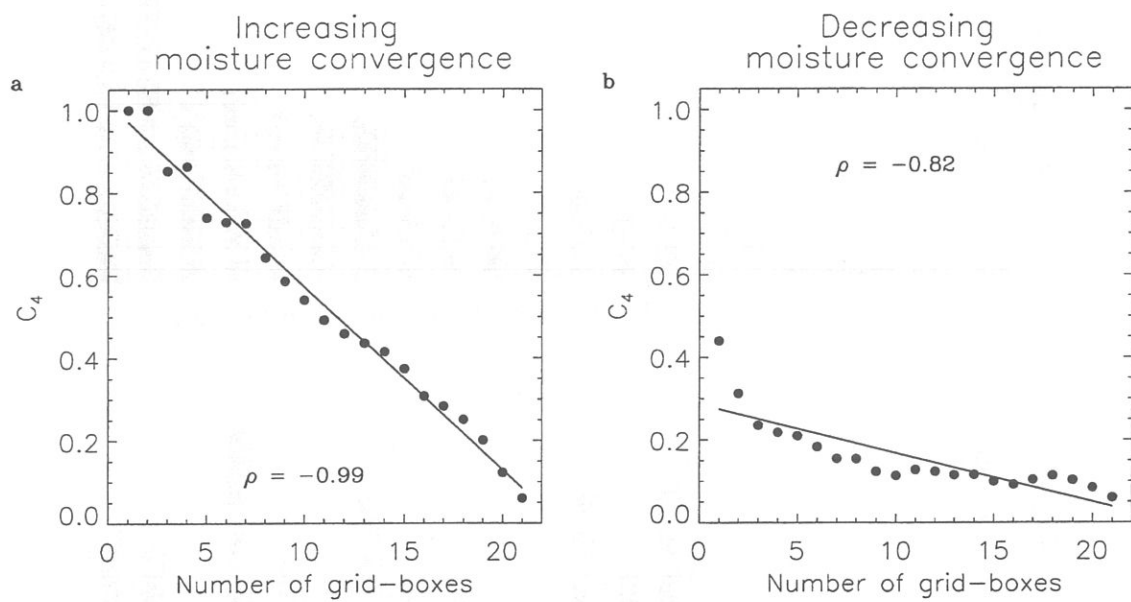


Figure 9: The Mississippi basin : coefficient C_4 for surface runoff against the number of aggregated grid-boxes ; aggregation following the order of **a** increasing, **b** decreasing, annual mean moisture convergence in DRN. A linear regression is drawn through the points, and ρ is the correlation coefficient.

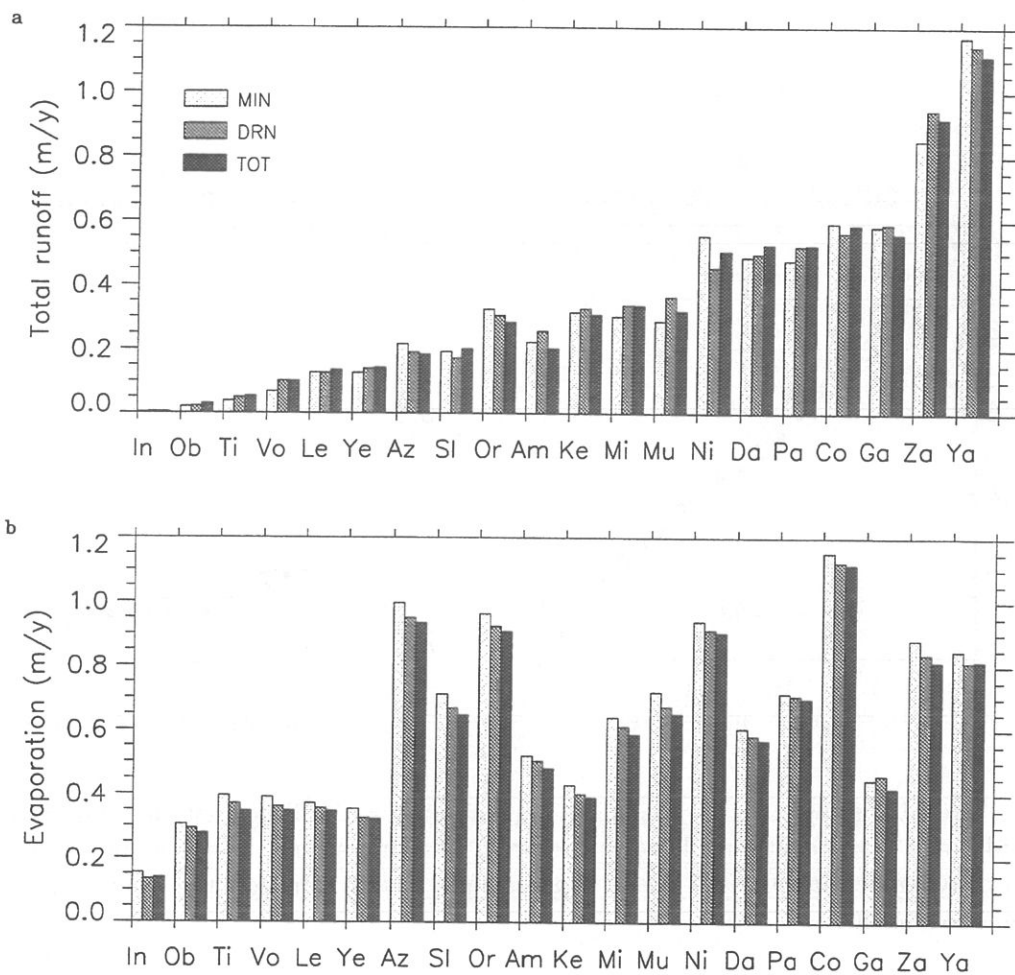


Figure 10: Comparison of DRN, TOT and MIN over 20 of the world largest river basins : annual means (per unit area, in m/year) of **a** total runoff and **b** evaporation.

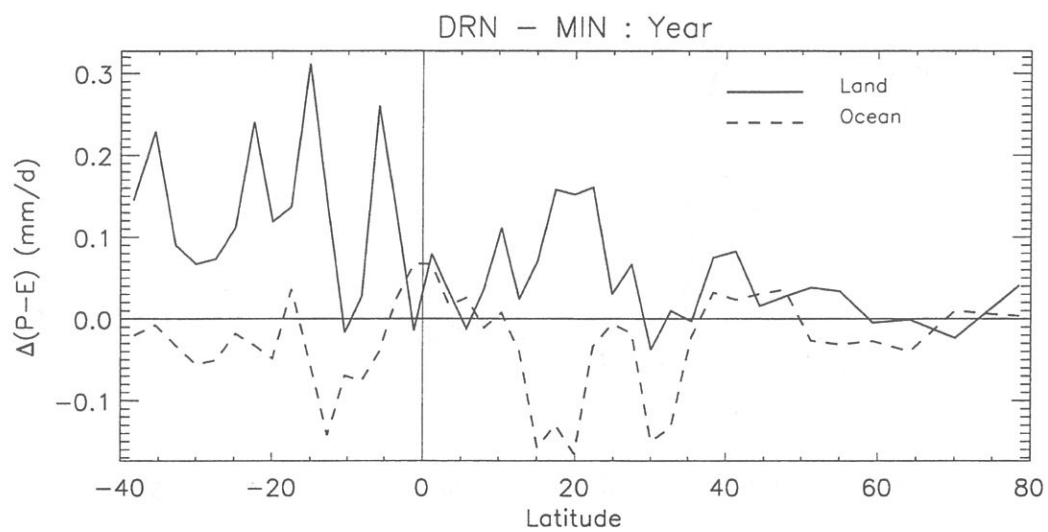


Figure 11: Year : zonal mean of the difference (DRN - MIN) in moisture convergence (mm/d) over land and oceans.

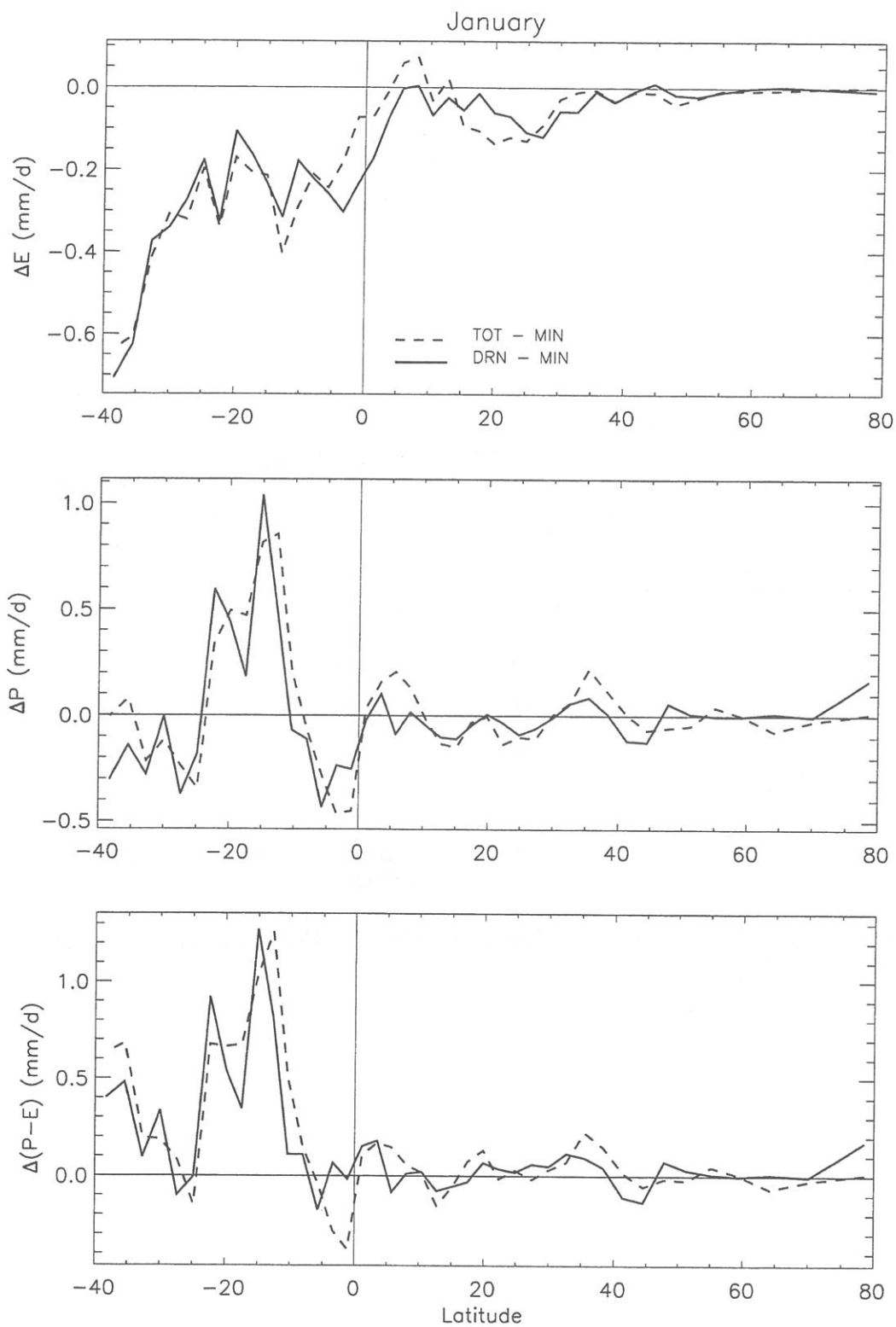


Figure 12: January : zonal means over land of the differences DRN-MIN and TOT-MIN (mm/d), in **a** evaporation, **b** precipitation and **c** moisture convergence.

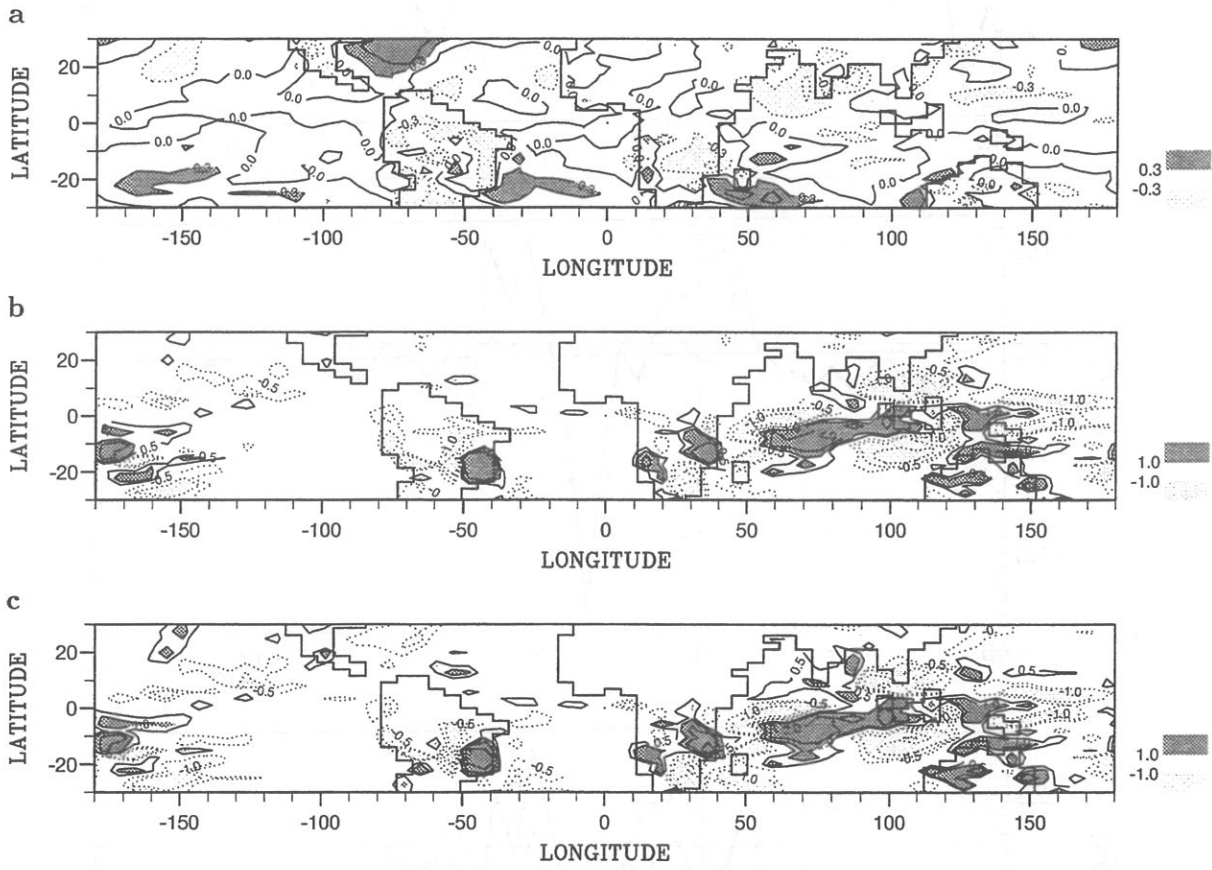


Figure 13: January : differences (DRN - MIN) in mm/d for **a** evaporation : contours at -0.6, -0.3, 0, 0.3, 0.6 ; **b** precipitation and **c** moisture convergence : contours at -2, -1, -0.5, 0.5, 1, 2.

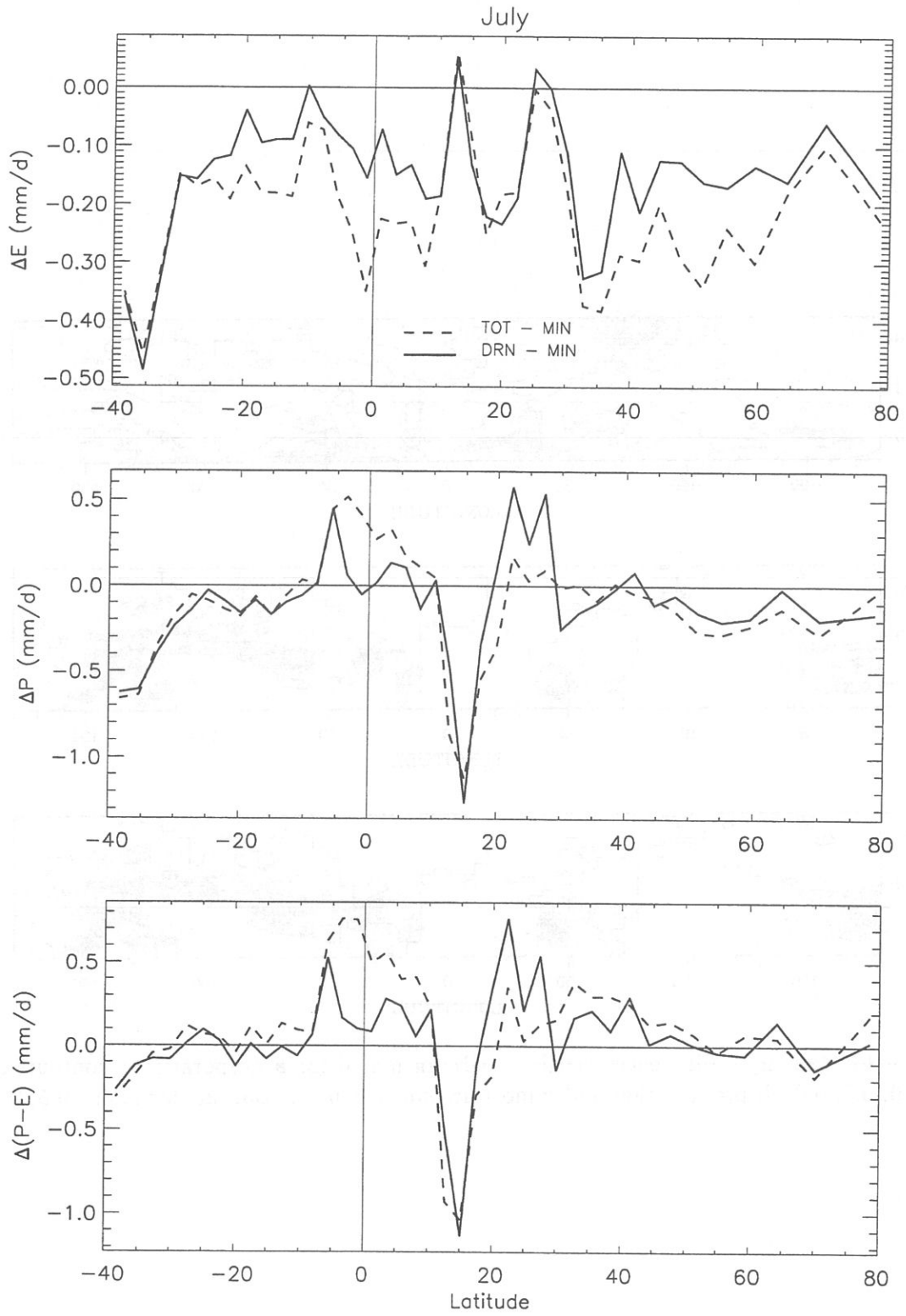
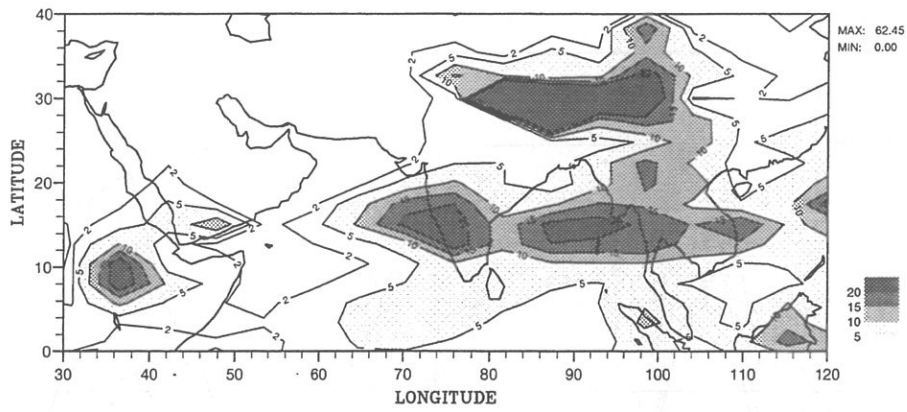
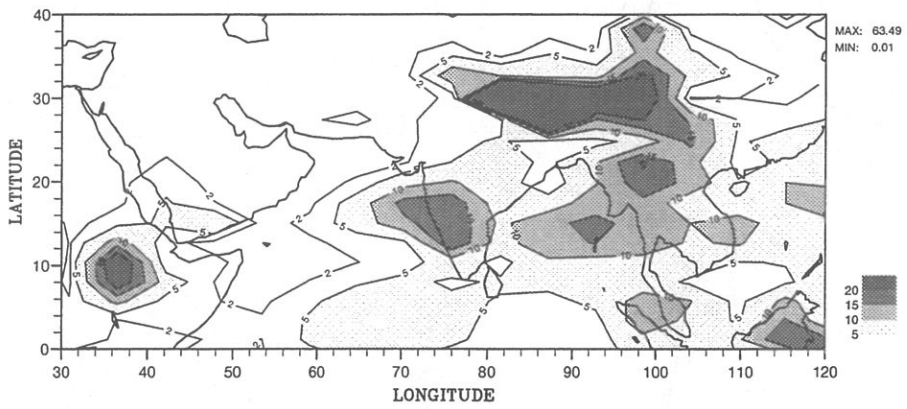


Figure 14: July : zonal means over land of the differences DRN-MIN and TOT-MIN (mm/d), in **a** evaporation, **b** precipitation and **c** moisture convergence.

a



b



c

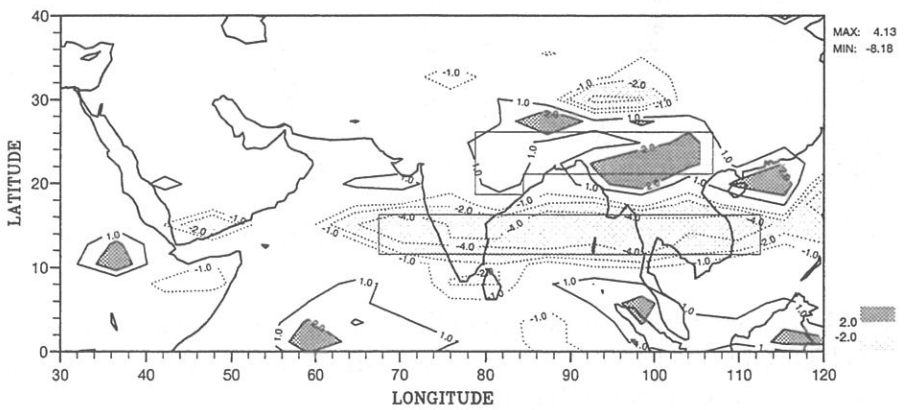


Figure 15: July : precipitation (mm/d) **a** in MIN and **b** in DRN ; contours at 2, 5, 10, 15, 20 , **c** difference (DRN-MIN) ; contours at -4, -2, -1, 1, 2, 4.

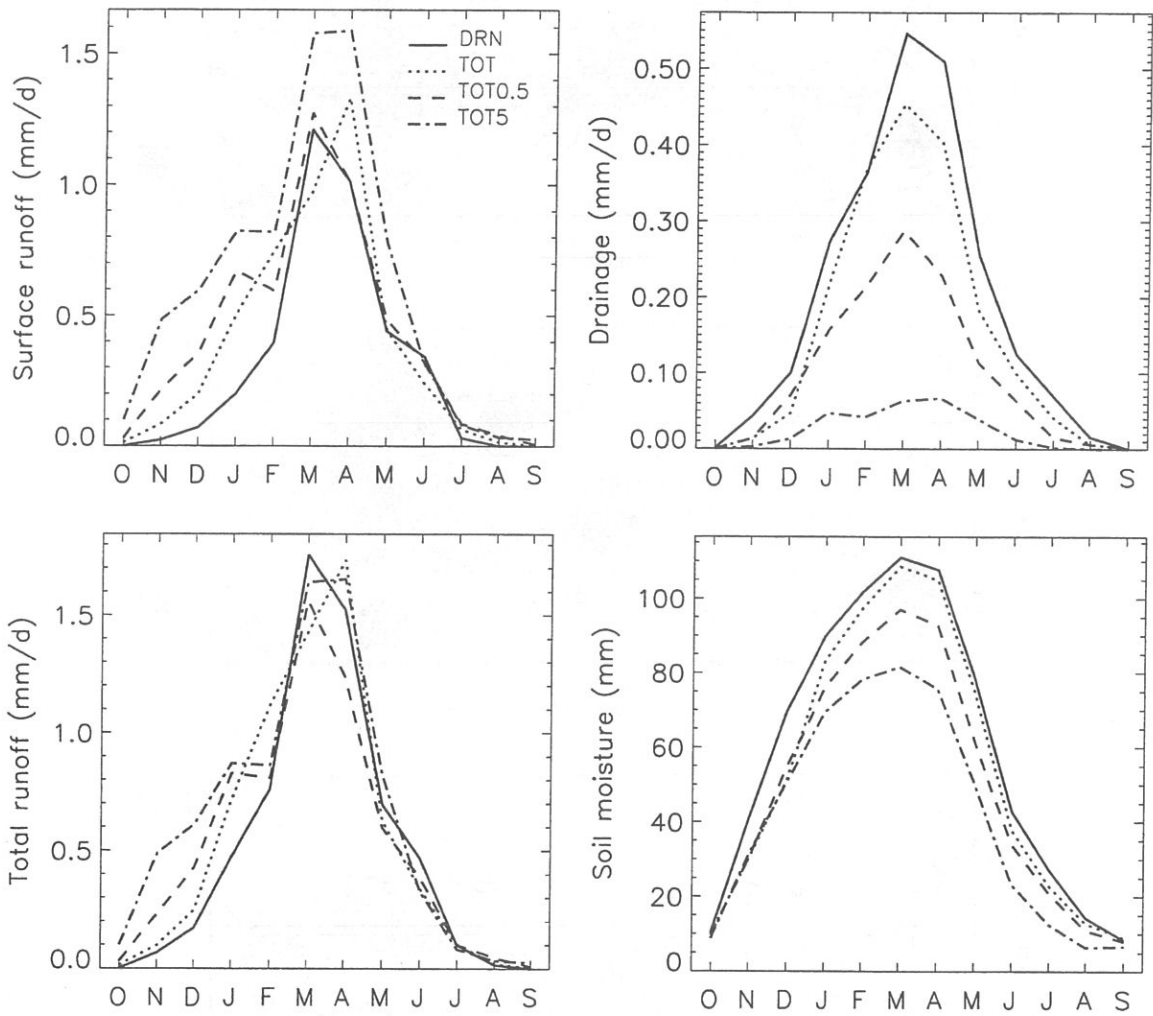


Figure 16: The Mississippi basin : mean annual cycles (monthly values, mm/d) simulated by DRN, TOT, TOT0.5 and TOT5, for surface runoff, drainage, total runoff and soil moisture. The time axis ranges from October to September.

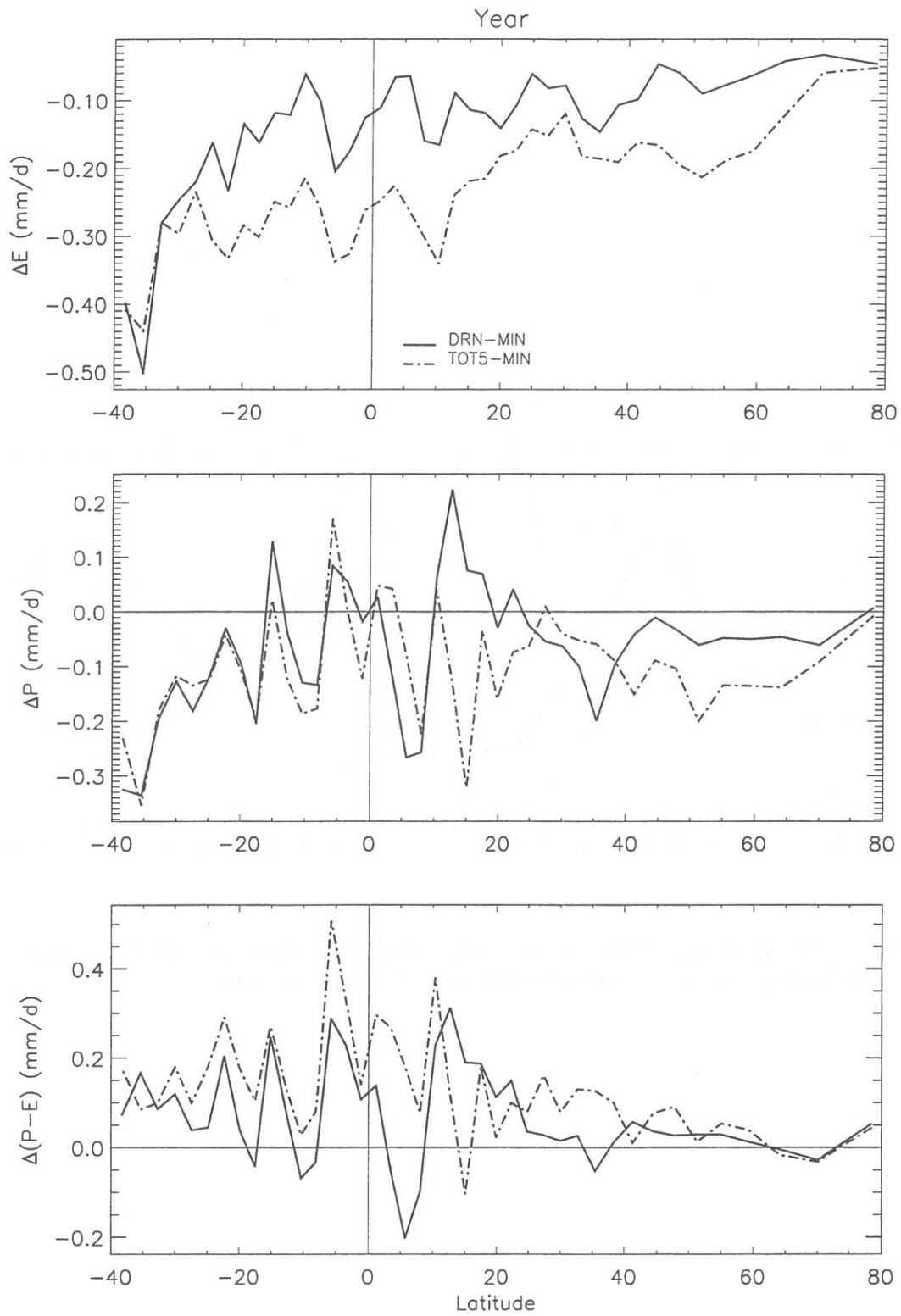


Figure 17: Annual zonal means over land of the differences DRN-MIN and TOT5-MIN, for **a** evaporation, **b** precipitation and **c** moisture convergence.

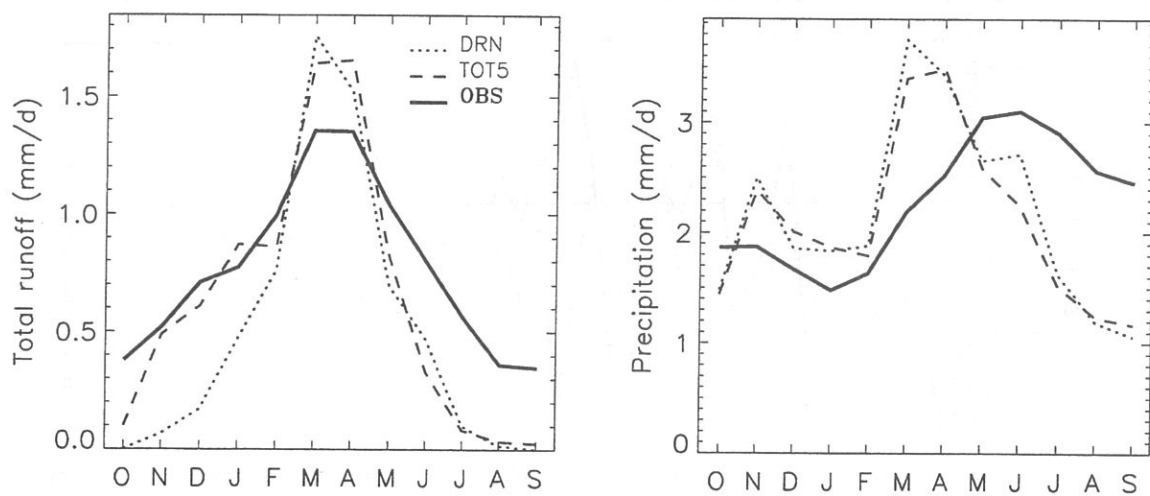


Figure 18: The Mississippi basin : comparison of simulated (DRN and TOT5) annual cycles of total runoff and precipitation with observed data (Wallis et al. 1991).

List of Tables

1	Comparison of the simulations MIN, DRN and TOT : annual means over all global land areas. A * indicates a statistically significant difference at the level $\alpha=0.05$. The differences between TOT and DRN on one hand, and MIN on the other one, are analyzed in section 5.	50
2	Twenty of the world largest rivers : labels and full names, in alphabetical order.	51
3	Comparison of the continental water budgets simulated by MIN, DRN, TOT, TOT0.5 and TOT5 (4-year annual means).	52
4	Estimates of the world water balance, per unit area (mm/year). P, E and Y denote precipitation, evaporation and total runoff, and C and O denote the continents and oceans.	53

Table 1: Comparison of the simulations MIN, DRN and TOT : annual means over all global land areas. A * indicates a statistically significant difference at the level $\alpha=0.05$. The differences between TOT and DRN on one hand, and MIN on the other one, are analyzed in section 5.

	MIN	DRN	TOT	TOT-DRN	DRN-MIN	TOT-MIN
Surface runoff (mm)	-	403	421	18	-	-
Drainage (mm)	-	99	82	-17*	-	-
Total runoff (mm)	480	502	503	1	22	23*
Soil moisture (mm)	62.2	57.1	53.6	-3.5*	-5.1*	-8.6*
Evaporation (mm)	566	527	518	-9*	-39*	-48*
Precipitation (mm)	1047	1029	1021	-8	-18	-26
Surface temperature (C)	14.0	14.3	14.5	0.2	0.3*	0.5*

Table 2: Twenty of the world largest rivers : labels and full names, in alphabetical order.

Label	Full name	Label	Full name
Am	Amur	Ni	Niger
Az	Amazon	Ob	Ob
Co	Congo	Or	Orinoco
Da	Danube	Pa	Parana
Ga	Ganges	Sl	St. Lawrence
In	Indus	Ti	Tigris-Euphrates
Ke	Mackenzie	Vo	Volga
Le	Lena	Ya	Yangtze
Mi	Mississippi	Ye	Yenisei
Mu	Murray	Za	Zambezi

Table 3: Comparison of the continental water budgets simulated by MIN, DRN, TOT, TOT0.5 and TOT5 (4-year annual means).

	MIN	DRN	TOT	TOT0.5	TOT5
Surface runoff (mm)	481	400	418	439	489
Drainage (mm)	-	100	82	66	33
Total runoff (mm)	481	500	500	505	522
Soil moisture (mm)	62	57	54	51	44
Evaporation (mm)	562	523	516	507	489
Precipitation (mm)	1045	1024	1016	1012	1008
Moisture convergence (mm)	483	501	500	505	522

Table 4: Estimates of the world water balance, per unit area (mm/year). P, E and Y denote precipitation, evaporation and total runoff, and C and O denote the continents and oceans.

References	P_C	E_C	Y	P_O	E_O	$E_O - P_O$
Baumgartner and Reichel (1975)	746	480	266	1066	1176	110
Budyko (1978)	800	450	350	1270	1400	130
Henning (1989)	718	442	276	1047	1159	112

